# Korozijsko ponašanje nehrđajućih čelika u morskoj vodi

**Matošin, Ante**

**UNIVERSITY OF SPLIT**

**FACULTY OF CHEMISTRY AND TECHNOLOGY**

# CORROSION BEHAVIOUR OF STAINLESS STEEL IN SEAWATER

**DIPLOMA THESIS**

**ANTE MATOŠIN**

**Parent number: 321**

**Split, October 2022.**

**SVEUČILIŠTE U SPLITU**

**KEMIJSKO-TEHNOLOŠKI FAKULTET**

**DIPLOMSKI STUDIJ KEMIJSKE TEHNOLOGIJE**

**SMJER: MATERIJALI**

# KOROZIJSKO PONAŠANJE NEHRĐAJUČEG ČELIKA U MORSKOJ VODI

**DIPLOMSKI RAD**

**ANTE MATOŠIN**

**Matični broj: 321**

**Split, listopad 2022.**

**UNIVERSITY OF SPLIT**

**FACULTY OF CHEMISTRY AND TECHNOLOGY**

**GRADUATE STUDY OF CHEMICAL TECHNOLOGY**

**ORIENTATION: MATERIALS**

# CORROSION BEHAVIOUR OF STAINLESS STEEL IN SEAWATER

**DIPLOMA THESIS**

**ANTE MATOŠIN**

**Parent number: 321**

**Split, October 2022.**

**TEMELJNA DOKUMENTACIJSKA KARTICA**

**DIPLOMSKI RAD**

**Sveučilište u Splitu, Kemijsko-tehnološki fakultet**
**Diplomski studij Kemijske tehnologije**
**Smjer: Materijali**

**Znanstveno područje:** Tehničke znanosti
**Znanstveno polje:** Kemijsko inženjerstvo
**Tema rada je prihvaćena** na 25. izvanrednoj sjednici Fakultetskog vijeća Kemijsko-tehnološkog fakulteta u Splitu održanoj dana 18. ožujka 2022. godine.

**Mentor:** Prof. dr. sc. Ladislav Vrsalović
**Pomoć pri izradi:**

# KOROZIJSKO PONAŠANJE NEHRĐAJUČEG ČELIKA U MORSKOJ VODI

Ante Matošin, 321

**Sažetak:**
Utjecaj temperature i koncentracije sulfidnih iona na korozijsko ponašanje nehrđajućih čelika 304L i 316L u morskoj vodi istraživan je različitim elektrokemijskim metodama. Tijekom istraživanja korištena su mjerenja potencijala otvorenog kruga, metode linearne i potenciodinamičke polarizacije. Utvrđeno je da se brzina korozije povećava s povećanjem temperature morske vode, a također i koncentracije sulfidnih iona. Analiza površine svjetlosnim mikroskopom i optičkim profilometrom nakon mjerenja potenciodinamičke polarizacije otkrila je da se broj i dubina jamica također povećavaju na isti način.

**Ključne riječi:** nehrđajući čelik, korozija, elektrokemijske metode, svjetlosna mikroskopija, profilometrijska analiza

**Rad sadrži:** 62 stranice, 47 slika, 8 tablica, 59 literaturnih referenci

**Jezik izvornika:** engleski

**Sastav povjerenstva za obranu:**

| | |
|---|---|
| 1. Prof. dr. sc. Nediljka Vukojević Medvidović | predsjednik |
| 2. Doc. Dr. sc. Miće Jakić | član |
| 3. Prof. dr. sc. Ladislav Vrsalović | mentor |

**Datum obrane:** 28. 10. 2022.

**Rad je u tiskanom i elektroničkom (pdf format) obliku pohranjen** u knjižnici Kemijsko-tehnološkog fakulteta u Splitu, Ruđera Boškovića 35.

**BASIC DOCUMENTATION CARD**

**DIPLOMA THESIS**

**University of Split**
**Faculty of Chemistry and Technology**
**Graduate study of Chemical Technology**
**Orientation: Materials**

**Scientific area:** Technical Sciences
**Scientific field:** Chemical Engineering
**Thesis subject was approved** by the Faculty Council of the Faculty of Chemistry and Technology, Session No. 25 which was held on March 18, 2022.

**Mentor:** Ph.D. Ladislav Vrsalović, Full prof.
**Technical assistance:**

# CORROSION BEHAVIOUR OF STAINLESS STEEL IN SEAWATER

Ante Matošin, 321

**Abstract:**
The effect of temperature and concentration of sulphide ions on the corrosion behaviour of 304L and 316L stainless steels in seawater has been investigated by different electrochemical methods. Open circuit potential measurements, linear and potentiodynamic polarization methods have been employed during the investigation. It has been found that the corrosion rate increases with the seawater's increasing temperature and the concentration of sulphide ions. Surface analysis with a light microscope and optical profilometer after potentiodynamic polarization measurements reveal that the number and depth of pits also increase in the same way.

**Keywords:** stainless steel, corrosion, electrochemical methods, light microscopy, profilometry analysis

**Thesis contains:** 62 pages, 47 figures, 8 tables, 59 references

**Original in:** English

**Defence Committee:**

1. Ph. D. Nediljka Vukojević Medvidović, Full Professor — chairperson
2. Ph. D. Miće Jakić, Assistant Professor — member
3. Ph. D. Ladislav Vrsalović, Full Professor — mentor

**Defence date:** 28. 10. 2022.

**Printed and electronic (pdf format) version of the thesis is deposed** in the Library of Faculty of Chemistry and Technology in Split, Ruđera Boškovića 35.

*This thesis was made at the Department of Electrochemistry and Materials Protection, at the Faculty of Chemistry and Technology in Split, under the supervision of Ph. D. Ladislav Vrsalović, Full professor, from June to October.*

*Sincere thanks to my mentor, Ph.D. Ladislav Vrsalović, Full professor, for his incredible help and for the time he dedicated during the making of this thesis. Many thanks to Ph.D. Jure Krolo, postdoctoral researcher at the Faculty of Electrical Engineering, Mechanical Engineering, and Naval Architecture, University of Split, for his help in the 3D profilometry research of the samples.*

*I owe an incredible dept to my mother and brother, who supported me at every step and ensured that I have everything that I need in order to reach this point. For that I am eternally grateful.*

# DIPLOMA THESIS ASSIGNMENT

1. To investigate the corrosion behaviour of AISI 304L and AISI 316L stainless steel in seawater at temperatures of 15 ℃, 25 ℃, and 35 ℃ by measuring the open circuit potential ($E_{OC}$), polarisation resistance ($R_p$) using linear polarization methods, and by determining the corrosion current density and corrosion potential from the potentiodynamic polarization curves.

2. After potentiodynamic polarization measurements, to examine corroded steel surfaces with a light microscope.

3. Using an optical profilometer, to determine the 3D topography and the width and depth of characteristics pits on the surface.

# SAŽETAK

Utjecaj temperature i koncentracije sulfidnih iona na korozijsko ponašanje nehrđajućih čelika 304L i 316L u morskoj vodi istraživan je različitim elektrokemijskim metodama. Tijekom istraživanja korištena su mjerenja potencijala otvorenog kruga, metode linearne i potenciodinamičke polarizacije. Utvrđeno je da se brzina korozije povećava s povećanjem temperature morske vode, a također i koncentracije sulfidnih iona. Analiza površine svjetlosnim mikroskopom i optičkim profilometrom nakon mjerenja potenciodinamičke polarizacije otkrila je da se broj i dubina jamica također povećavaju na isti način.

**Ključne riječi:** nehrđajući čelik, korozija, elektrokemijske metode, svjetlosna mikroskopija, profilometrijska analiza

# SUMMARY

The effect of temperature and concentration of sulphide ions on the corrosion behaviour of 304L and 316L stainless steels in seawater has been investigated by different electrochemical methods. Open circuit potential measurements, and linear and potentiodynamic polarization methods, have been employed during the investigation. It has been found that the corrosion rate increases with the increasing seawater's increasing temperature and concentration of sulphide ions. Surface analysis with a light microscope and optical profilometer after potentiodynamic polarization measurements reveal that the number and depth of pits also increase in the same way.

**Keywords:** stainless steel, corrosion, electrochemical methods, light microscopy, profilometry analysis

# CONTENTS

# INTRODUCTION

Iron represents one of the most influential and widely used engineering materials, however, it is rarely used in its elemental form, but rather in combination with other elements. Mixtures of iron and additional elements are called ferrous/iron alloys and are classified according to their carbon content. Ferrous alloys with a carbon content between 0.08-2 wt. % are called steels. Steels can be further categorized based on their chemical composition into low alloy, or carbon steels and high alloy steels.[1] Although iron alloys represent some of the most widely used engineering materials, they are also the least corrosive resistant, as they rust in air, corrode in acids and scale in high-temperature atmospheres. To improve the stability of steels in such conditions, higher chromium content is introduced. The resulting alloy is called 'stainless steel' due to its high corrosion resistance[2,3]. However, even with a high content of Cr and the addition of other beneficial elements, stainless steels are never completely resistant to corrosion. When exposed to an environment that damages, reduces, or inhibits the formation of the passive film, the corrosion resistance of the alloy becomes compromised.

There are several characteristic forms of stainless-steel corrosion, each with a different driving force. However, they all have a common causing factor that is crucial to the corrosion resistance of all stainless-steel grades. That common factor is the presence of halides, of which chlorides are most represented in practice.[4] Consequently, when it comes to corrosive mediums, seawater is one of the most destructive, as it's the only natural electrolyte containing a relatively high concentration of chlorides. Beside the intensive impact of chlorides and other halide ions naturally present in seawater, pollutants can also have a high influence on the corrosion of metals. Human and industrial activities increase the generation of $CO_2$, $H_2S$ and $NH_3$, which can in turn increase the corrosion rate of construction materials.

The aim of this paper is to investigate the corrosion behaviour of AISI 304L and AISI 316L stainless steel in fresh and sulphide polluted seawater at temperatures of 15 ℃, 25 ℃, and 35 ℃ through electrochemical methods of analysis and by examining corroded steel surfaces with a light microscope and an optical profilometer.

# 1. THEORETICAL OVERVIEW

## 1.1. Iron

From the Stone Age to the present age of polymers and composites, human progress has been made possible by the mastery of engineering materials and their properties. However, there is one material that has arguably had the greatest impact on the development of modern civilisation.

Iron (Latin: *Ferrum*) is one of the most influential and widely used engineering materials, especially in the form of alloys with carbon and other metals. It is a transition metal of greyish colour belonging to the 8th group of the periodic table and has an atomic weight of 55.845 and an atomic number of 26. Together with nickel and cobalt, it forms the so-called iron triad. All three of these metals tend to passivate and have ferromagnetic properties. Furthermore, iron represents one of the most abundant elements in nature, accounting for about 5% of the total mass of the Earth's crust, mainly in the form of oxide, carbonate, silicate, and sulphide minerals.[5]

***Figure 1*** Prehistoric beads made from meteoritic iron.[6]

The earliest evidence of the use of iron dates back to 3500 BC from Egypt, where iron beads originating from a meteorite were found.[7] Meteoric iron was highly regarded because of its celestial origin and was often used to forge weapons and tools.[8]

Meteoric iron is also the only natural source of elemental iron in the earth's crust, as iron reacts readily with oxygen and other gases under atmospheric conditions to form iron compounds (iron ore). In this way, early civilisations were able to use iron in its practical, metallic form long before technologies for extraction and refining were developed.

The aptly named Iron Age (1200 BC) began with the development of technologies for extracting and refining iron from ores. As these technologies became more available and easier to use, the use of iron materials became more widespread. The most remarkable historical increase in iron production occurred after the Industrial Revolution, due to the intensive mechanisation of production processes and the invention of new, faster forms of transport (especially locomotives and steamships), which required a strong and robust building material that could withstand the intense working conditions.

## 1.2. Ferrous alloys

Metallic materials are rarely used in their elemental form, but rather as a combination of base metal and other elements called alloys. Iron is the best-known example, as it is used almost exclusively in the form of iron alloys. Iron alloys, as engineering materials, are classified according to their carbon content. A mixture of iron and carbon that contains more than 2 % carbon is called cast iron. With increasing carbon content, iron becomes harder but less ductile. Therefore, cast iron is wear-resistant but also relatively brittle. Due to these properties, it cannot be used as a structural material, e.g., in bridge construction. For these applications, iron with a lower carbon content is used because it can be bent under load without breaking.[1]

## 1.3. Steel

Steel is a ferrous alloy with a carbon content between 0.08-2 wt. %, representing a balance between hardness and ductility. It is an extremely useful engineering material with excellent physical properties, as it offers strength, rigidity, durability, and it can be cut, shaped and joined.[1] The importance of steel can be best exemplified by the fact that the industrial development of a particular country is often measured through its per capita consumption of steel.

Modern steel production is based on two processes: refining of crude(pig) iron in oxygen converters and recycling scrap iron in electric arc furnaces. Since steel is 100% recyclable, it can be recycled infinitely into the same material without any loss in quality. In North America alone, 60 to 80 million tons of steel scrap are recycled yearly into new steel products.[9]

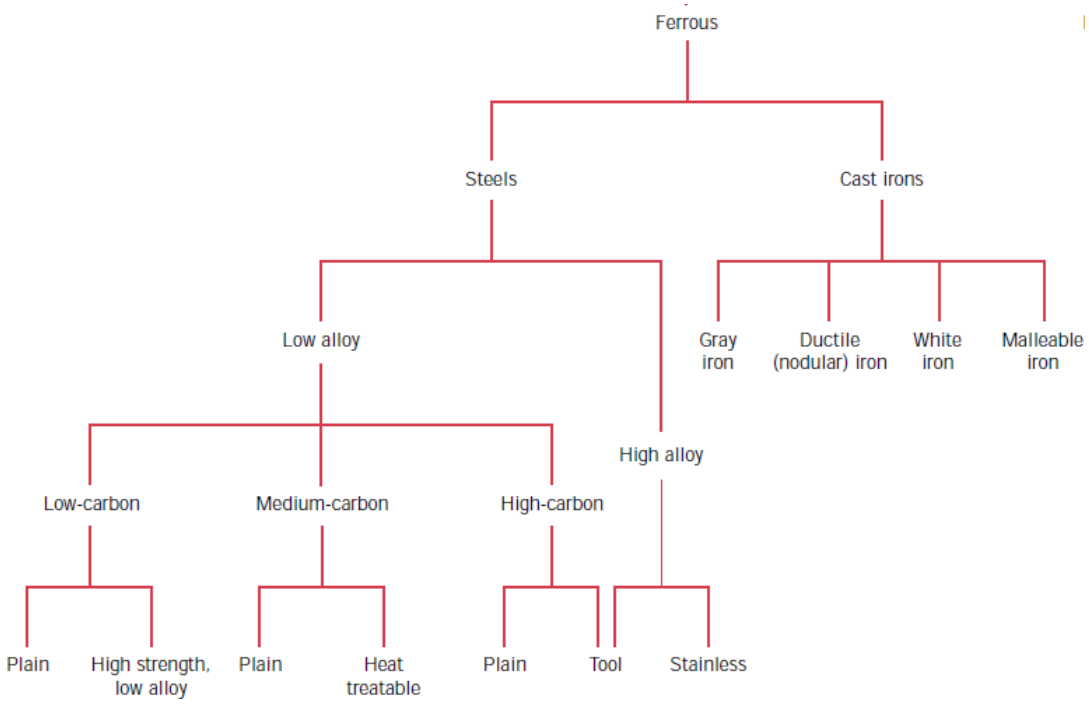


***Figure 2*** Classification of ferrous alloys.[10]

Steels are generally categorized based on their chemical composition. Accordingly, there are:

1. low alloy, or carbon steels
2. high alloy (stainless) steels

Low alloy or carbon steels, can again be divided into low, medium and high carbon steels, depending on their carbon content. Although they contain little to none of the other alloying metals present in high-alloy steels (generally less than 5 wt. %), they still contain elements such as Mn, Si, S, P and Al, which are needed to produce a structural material of desired quality.[11]

Low carbon steels contain less than 0.25 wt. % of carbon and are produced in the greatest quantity. They are unresponsive to heat treatments and are strengthened through cold working processes, such as cold rolling, hammering and spinning. Consequently, low carbon steels are relatively soft and weak, but very ductile, machinable, weldable and cheaper to produce compared to other steels.

Medium-carbon steels have a carbon content of 0.25 - 0.6 wt. %. They can be heat treated and are most often utilized in the tempered condition. The addition of other metals, such as Cr, Ni and Mo further improves the capacity for heat treatment.[7] These alloys are stronger compared to low-carbon steels, but at a sacrifice of toughness and ductility. Medium-carbon steels are often used in machine parts (crankshafts, gears) and high-strength structural components.

High carbon steels have a carbon content of 0.6-1.4 wt. %, which consequently makes them the hardest, the strongest, but also the least ductile of all the carbon steels. They are most frequently used in a hardened and tempered conditions. Often, additional metals are added, creating high-carbon alloys. Metals such as chromium, wolfram and molybdenum combine with the present carbon to create tough and resistant carbide compounds within the steel. Their resistance to wear and their capability to maintain a sharp edge makes them an ideal material for cutting tools and moulds for shaping and forming other materials.[10]

## 1.4. Stainless steel

Although ferrous alloys are the most widely used engineering materials, they are also the least corrosive resistant, as they rust in air, corrode in acids and scale in high-temperature atmospheres. To improve the stability of steels in such conditions, a higher chromium content (above 10.5 wt. % according to the European standard) is introduced, often accompanied by nickel and molybdenum. The resulting alloy is called ‘stainless steel’

due to its high resistance to corrosion, even when exposed to seawater, concentrated acids, or high temperatures.

Chromium is the main alloying element that gives stainless steel these properties. At a content of around 11 wt. %, it spontaneously reacts with oxygen in the surrounding atmosphere, forming a passive oxide layer on the steel's surface. This layer acts as a protective barrier between the metal construction and the surrounding atmosphere. The passive layer also has the ability of self-healing, ensuring anticorrosion protection even after suffering damage.[2]

There are many types of stainless steel with very different chemical compositions. However, the main criterion for categorization of stainless steels is their microstructure, as it plays a crucial role in their physical and mechanical properties. Microstructure, i.e., the crystal form of the base element, iron. Iron exhibits several allotropic modifications under specific conditions. At atmospheric pressure, three allotropic forms of iron exist.

The primary modification of iron is α-Fe, or ferrite, which is stable at temperatures below 910˚C and is characterized by a body-centred cubic (BCC) crystal structure. The second allotropic modification of iron is γ-Fe, or austenite. It is stable at temperatures above 910˚C and has a face-centred cubic (FCC) crystal structure. Above 1400 ˚C, iron transforms to BCC crystal structure called δ-Fe. Moreover, when austenitic modification in combination with carbon is rapidly cooled, an additional crystalline modification can be achieved. As a result of the rapid cooling (most commonly through quenching), carbon atoms do not have enough time to diffuse out of the crystal structure, and the austenite transforms into a body-centred tetragonal form (BCT) called martensite.[12]

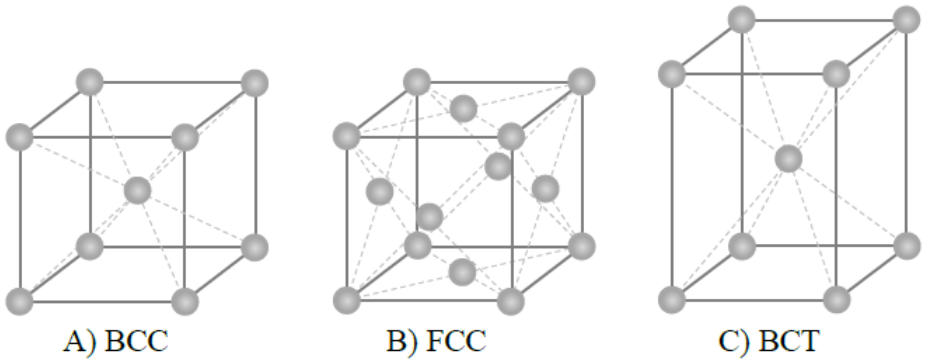


***Figure 3*** Crystal structure of A) ferritic, B) austenitic and C) martensitic stainless steels.[12]

Each of these modifications offers different solubility for carbon, and in combination with carbon (and other alloying elements), forms differing solid mixtures.

Accordingly, stainless steels are divided into four families:

1. ferritic stainless steels
2. austenitic stainless steels
3. martensitic stainless steels
4. ferritic-austenitic or duplex stainless steels

As an additional form of identification, stainless steels within each family are divided into grades. The grades are assigned to alloys that are commonly use in practice because of their properties. The primary function of the grades is to describe the properties of an alloy, such as toughness, magnetism, corrosion resistance and composition.[3]

For simplicity, various scientific and technical communities have developed standardised systems for classifying steels, such as AISI (American Iron and Steel Institute) and EN (European Standards).

***Table 1***. AISI grades of stainless steels.[3]

| AISI Designation | Main alloying elements; family; magnetic properties |
|---|---|
| 2xx | Cr-Ni-Mn; austenitic; nonmagnetic |
| 3xx | Cr-Ni; austenitic; nonmagnetic |
| 4xx | Cr; martensitic; magnetic |
| 4xx | Cr; ferritic; magnetic |

### 1.4.1. Ferritic stainless steels

According to the AISI system, ferritic steels are designated with the 4xx series. Standard ferritic stainless steels are alloyed with chromium, either with small amounts or without nickel. Nickel is one of the most expensive alloying elements in stainless steels, which is why ferritic stainless steels are among the least expensive.[4] They can contain Mo, Nb and Ti to improve their corrosion resistance and physical properties. Due to their ferritic microstructure, most steels in this family are magnetic and weld well. There are also high-temperature ferritic steels, which have increased resistance to high temperatures (800-1500 ˚C). They are often alloyed with more carbon to improve creep resistance, and also with silicon and aluminium for additional oxidation resistance.[4]

## 1.4.2. Austenitic stainless steels

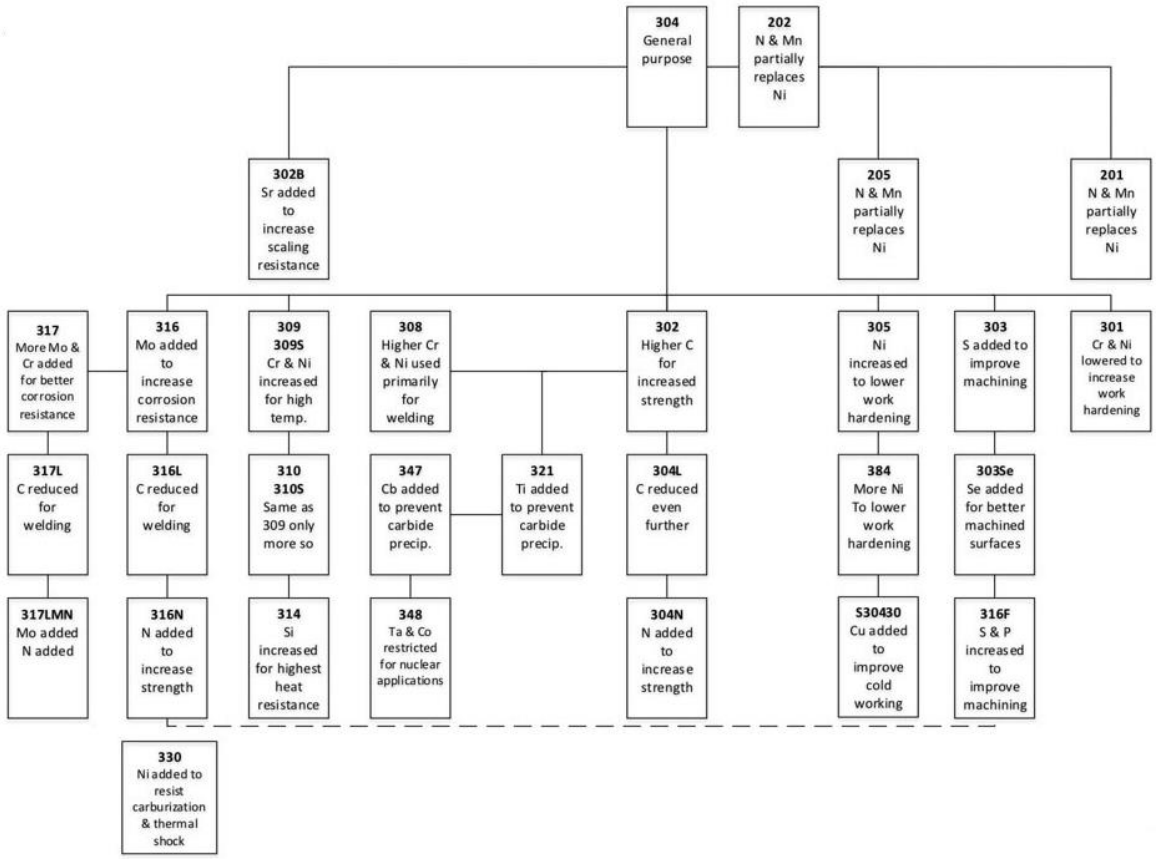


***Figure 4*** AISI grades of austenitic stainless steels, with their alloying elements and their effects on final properties.[3]

The austenitic family represents the largest and most widely used group of stainless steels. Typical chemical composition of these alloys is: Cr 16-18 wt. %, Ni 8-20 wt. %, C 0.03-0.15 wt. %. The primary function of Ni as an alloying element is to promote and stabilize the formation of an austenitic structure. Manganese, and nitrogen are also added to the alloy for the same purpose.[11]

Austenitic stainless steels belong to the AISI 2xx and 3xx series. They have good to excellent corrosion resistance, good formability, and weldability. Due to their microstructure, they do not exhibit magnetic properties. However, the strength of austenitic steels is often improved through cold working, resulting in the formation of martensite, which is magnetic.

AISI 304 and 316 grades of austenitic stainless steels are the most versatile and widely used in the 300 series. AISI 304 grades are the base steels of the austenitic family, with a Cr content of around 18 % by weight and a Ni content of around 8 wt. %. In addition to these elements, certain grades are alloyed with nitrogen and sulphur to improve their strength and machinability. They have good corrosion resistance in various atmospheres and are often used as a construction material for process equipment in the food industry and for the construction of chemical tanks, heat exchangers and pipelines.[13]

***Table 2*** Chemical composition of AISI 304 grades.[3]

| Grade | Range | Content of alloying elements / wt. % | | | | | | | | |
|---|---|---|---|---|---|---|---|---|---|---|
| | | C | Mn | Si | P | S | Cr | Mo | Ni | N |
| 304 | Min. | - | - | - | - | - | 18.00 | - | 8.00 | - |
| | Max. | 0.08 | 2.0 | 0.75 | 0.045 | 0.03 | 20.00 | - | 10.50 | 0.10 |
| 304L | Min. | - | - | - | - | - | 18.00 | - | 8.00 | - |
| | Max. | 0.03 | 2.0 | 0.75 | 0.045 | 0.03 | 20.00 | - | 12.00 | 0.10 |
| 304H | Min. | 0.04 | - | - | - | - | 18.00 | - | 8.00 | - |
| | Max. | 0.10 | 2.0 | 0.75 | 0.045 | 0.03 | 20.00 | - | 10.50 | - |

In comparison, AISI 316 grades have the advantage in terms of corrosion resistance. They are also referred to as Cr-Ni-Mo grades, and are described as ‘general purpose alloys’ with an improved corrosion resistance.[12] The 316 grades have a lower Cr content than the 304, around 17 wt. %, but have a Ni content of around 12 wt. %. Although nickel doesn’t have a direct impact on the formation of the passive layer, it improves the corrosion resistance of the alloy, especially in acidic conditions. The improved corrosion resistance of these grades is also attributed to the addition of 2-3 wt. % of Mo. Molybdenum has a synergistic interaction with Cr, increasing the stability of the passive oxide layer and the resistance to pitting corrosion in hydrochloric acid, diluted sulfuric acid and in solutions containing chlorides.[14]

It should be noted that the interactions between the alloying elements are incredibly complex and many of them are still unclear. The effects of the main elements (Cr, Ni) on the final properties, such as phase equilibrium and corrosion resistance have been well studied, while the effect of less represented alloying elements and their interactions with each other are still under investigation. Manganese, for example, was regarded as both an austenitiser and a ferritiser.

It was later suggested that its effect on phase equilibrium depends on its content, behaving like the former at lower levels and like the latter at higher levels. The complicated role of Mn was also confirmed by later investigations on Cr-Mn stainless steels, which showed its complex interaction with other alloying elements (Cr, Ni, N, C, ...).[15]

### 1.4.3. Martensitic stainless steels

Martensitic steels are the smallest group of stainless steels. They are produced by quenching steels with a lower Cr/C quotient after hot working and before heat treatment.[16] They belong to the AISI 4xx series, of which grades 403, 410 and 420 are the best known. Martensitic stainless steels typically contain 12-18 wt.% Cr and 0.15-1.2% C. They have a higher carbon content to improve their strength and hardenability. Their corrosion behaviour is similar to that of ferritic grades, although they are less prone to intergranular corrosion.[13] They are resistant to water and weaker organic acids, but are prone to hydrogen embrittlement, especially in the presence of sulphides. Therefore, martensitic grades are used in conditions where low corrosion resistance is required, especially in the construction of hydroelectric turbines, pumps, valves and medical equipment.[17]

### 1.4.4. Duplex stainless steels

Duplex stainless steels are defined as alloys with a mixed microstructure of austenite and ferrite. This mixed microstructure is a major advantage over other conventional stainless steels, as each phase imparts beneficial properties to the alloy.[18]

The ferritic structure enables duplex steels very good resistance to stress corrosion cracking, while the austenitic structure provides better ductility and toughness. During production, the aim is to obtain equal amounts of austenite and ferrite through controlled heat treatment and the addition of certain alloying elements.[14]

Regarding their composition, duplex steels are characterized by high chromium content, at around 20.1-25.4 wt. %, and relatively low nickel content, ranging between 1.4-7 wt. %. Consequently, they are incredibly resistant to corrosion, particularly in the presence of chlorides and sulphides.[14]

Molybdenum and nitrogen are also added to these alloys to further improve corrosion resistance and strength. Due to their increased yield strength, thinner sections of duplex stainless steels can be produced, resulting in significant weight savings. This makes duplex stainless steel a popular choice for structural applications and pressure vessels.[19]

During the 1980's, as part of the duplex group of stainless steels, new alloys with even better resistance to localized corrosion were developed to withstand more aggressive environments. These grades approximately contain 25 wt.% Cr, 6-7 wt. % Ni, 3-4 wt. % Mo, 0.2-0.3 wt. % N, 0-2 wt. % Cu and 0-2 wt. % W. Thanks to their composition and properties, these alloys are often called super-duplex stainless steels. They offer incredible resistance to acids, chlorides and other aggressive environments.[18]

***Table 3*** Chemical composition of AISI duplex stainless-steel grades.[4]

| Grade | Range | Content of alloying elements / wt. % | | | | | | | | |
|---|---|---|---|---|---|---|---|---|---|---|
| | | C | Si | Cu | S | Cr | Mo | Ni | Mn | N |
| 2205 | Min. | - | - | 3.00 | - | 21.00 | 2.50 | 4.50 | - | 0.05 |
| | Max. | 0.03 | 1.00 | 5.00 | 0.03 | 23.00 | 3.50 | 6.50 | - | 2.00 |
| 2304 | Min. | - | - | 0.04 | - | 21.00 | 2.50 | 3.00 | - | 0.05 |
| | Max. | 0.03 | 1.00 | 2.00 | 0.03 | 24.50 | 3.50 | 3.50 | 2.50 | 2.00 |
| 2507 | Min. | - | - | - | - | 24.00 | 3.00 | 6.00 | - | 0.24 |
| | Max. | 0.03 | 0.80 | 0.50 | 0.02 | 26.00 | 5.00 | 8.00 | 1.2 | 0.32 |

## 1.5. Corrosion

Corrosion (Lat. *corrodere* - 'to gnaw through') is a natural process through which a material gradually deteriorates under the physical, chemical and biological influences of its environment. In technical terms, it applies both to metallic and non-metallic materials. However, it is more often used in the context of metals, while for non-metallic materials, terms like degradation and decomposition are used. According to the ISO 8044:1999 norm, "corrosion results in changes in the properties of the metal, which may lead to significant impairment of the function of the metal, the environment, or the technical system, of which these form a part".

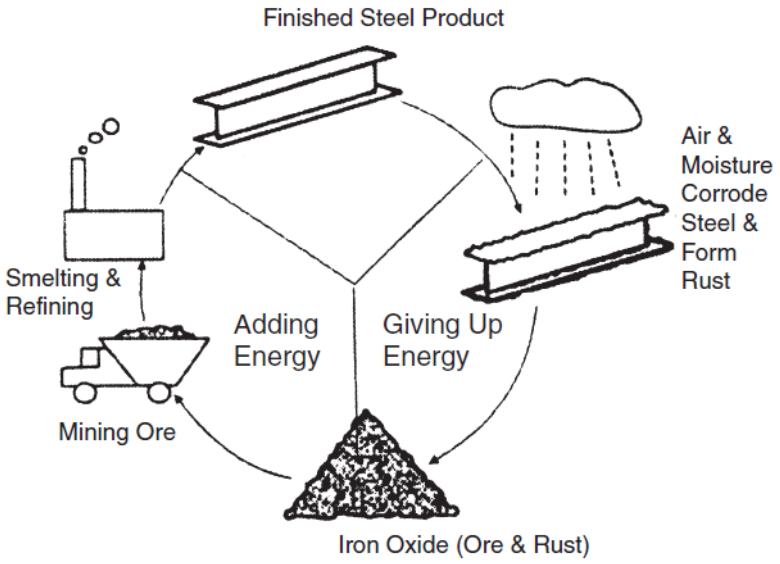


***Figure 5*** Corrosion cycle of steel.[20]

Corrosion, like all natural processes, is caused by the tendency of all systems towards lower energy states. An example of such tendency is shown in *Figure 5*, which depicts the corrosion cycle of steel. Because of the atmospheric conditions, iron can be found in nature almost exclusively in the form of iron ore. To be used in a practical manner, it is extracted from its ore and refined into its metallic form, bringing it to a higher energy state. Gradually, the metallic iron, as the base component of steel, reacts with oxygen and water (both of which are present in most natural environments) and transforms into various corrosion products. These corrosion products represent the equilibrium state of lower energy, and their chemical composition is very similar to the original iron ore.[20]

The rate and extent of corrosion is dependent on the conditions of the surrounding environment and characteristics of the material (composition, structure, surface). Thus, corrosion can be defined as a process through which a system is trying to achieve its lowest energy state under given conditions. It is spontaneous, and consequently characterized with a decrease in Gibbs energy ($\Delta G < 0$).[21]

Corrosion processes are commonly classified according to the:

1. process mechanism: chemical and electrochemical
2. environment: atmospheric, soil, water, …
3. type of attack: general, local, selective, intergranular, …[22]

### 1.5.1. Chemical and electrochemical corrosion

Chemical corrosion can be defined as a chemical reaction between a metal and molecules of an element or a compound in non-electrolytic solutions or dry hot gasses, resulting in the oxidation of the metal. It involves direct charge transfer between the metal atom and the oxidising species. An example of chemical corrosion would be the reaction between a metal and oxygen gas. The reaction results in the formation of metal oxides, which represent the corrosion products.

$$xMe + \frac{y}{2}O_2 \rightarrow Me_xO_y \quad (1)$$

On the other hand, electrochemical corrosion represents a process that unfolds in electrolytic mediums, and which consists of two half-reactions, oxidation and reduction. It is the most widespread form of corrosion, accounting for 95% of all corrosion processes.

The electrochemical nature of these processes can be illustrated through the interaction between hydrochloric acid and zinc. When zinc is submerged in a diluted solution of hydrochloric acid, a reaction occurs, resulting in the generation of hydrogen gas, dissolution of zinc metal, and formation of zinc chloride.[23] Because chloride ions do not take part in the main process, the reaction can be written as:

$$Zn + 2H^+ \rightarrow Zn^{2+} + H_2 \quad (2)$$

The same reaction can be separated into two half-reactions which occur at the metal surface:

a) oxidation of Zn:

$$Zn \rightarrow Zn^{2+} + 2e^{-} \tag{3}$$

b) reduction of hydrogen ions:

$$2H^{+} + 2e^{-} \rightarrow H_2 \tag{4}$$

During electrochemical corrosion, more than one oxidation and one reduction reaction may occur. In case of the corrosion of an alloy, any of its component metal atoms can be oxidized. Additionally, more than one reduction reaction can take place on the surface of a metal. If we again examine the corrosion of zinc in a hydrochloric acid solution, this time, however, containing dissolved oxygen, besides the evolution of hydrogen, illustrated in *Equation 4*, reduction of oxygen also occurs. In acidic conditions the reaction can be written as follows:

$$O_2 + 4H^{+} + 4e^{-} \rightarrow 2H_2O \tag{5}$$

Furthermore, now that there are two reduction reactions or processes which consume electrons, the overall corrosion rate of zinc is increased.[24]

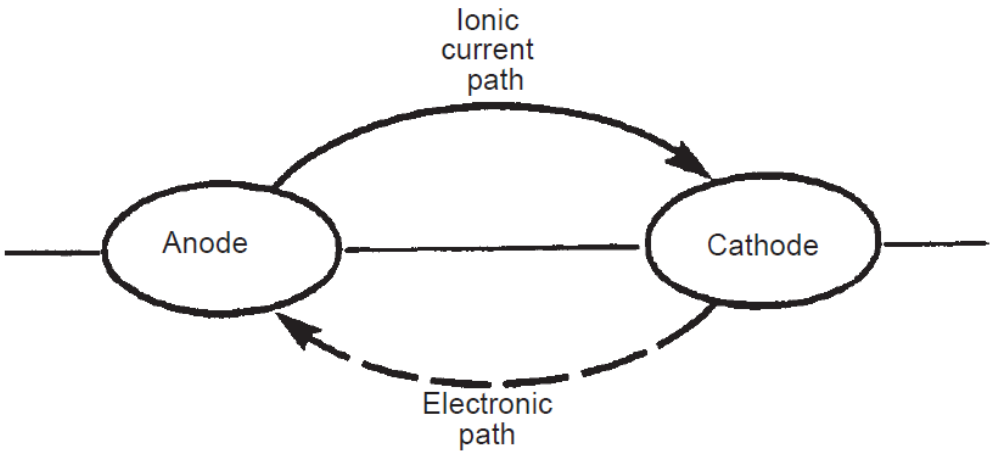


***Figure 6*** Depiction of an electrochemical corrosion cell.[20]

The region of metal at which oxidation occurs (releasing of electrons) is called the anode. It is where metal atoms transfer into the solution in the form of ions, resulting in mass loss, or rather in the actual corrosion of the metal. The region at which reduction occurs (binding of electrons) is called the cathode. At the cathode, no weight loss occurs, however, the reduction reactions that take place there are just as significant for the operation of the corrosion cell.

These areas are the result of local potential differences caused by inhomogeneities in the metal surface, structure, internal and external stresses, uneven flow of the surrounding fluid, differences in temperature, etc.[20]

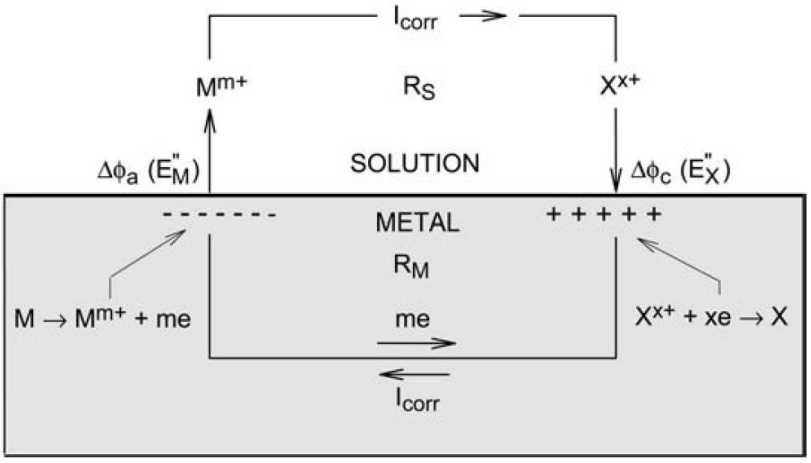


***Figure 7*** Schematic depiction of an electrochemical corrosion cell.[25]

As part of the corrosion process, there is a transfer of electrons and ions through the metal/electrolyte interface and between the cathode and the anode (*Fig. 7*). The direct current (flow of positive electric charge) going through the corrosion cell enters the solution through the anode. It then flows through the solution, from the anode to the cathode, by the movement of charged ions. After reaching the cathodic region, the current enters the metal, and through the electronic path travels back to the anode, closing the corrosion cell.[20,25]

The current going through the corrosion cell is the corrosion current $I_{corr}$, and according to the Ohm's law is equal to:

$$I_{corr} = \frac{(E_M - E_X)}{(R_S + R_M)} \quad (6)$$

where:
- $\boldsymbol{I_{corr}}$ - corrosion current [A]
- $\boldsymbol{E_M}$ - anodic interface potential difference [V]
- $\boldsymbol{E_X}$ - cathodic interface potential difference [V]
- $\boldsymbol{R_S}$ - solution path resistance [Ω]
- $\boldsymbol{R_M}$ - metal path resistance [Ω]

$I_{corr}$ is a measure of the total loss of metal from the anode surface during corrosion and is equal to the anodic and cathodic currents. Anodic and cathodic currents are proportional to the rates of oxidation and reduction reactions. During corrosion, the rates of oxidation and reduction are the same and there is no accumulation of charges on the corroding surface. Thus, absolute anodic and cathodic currents are also equal, $I_a = I_c = I_{corr}$.[25]

To conclude, in order to operate, an electrochemical corrosion cell must fulfil four requirements:

anode
cathode
electrolyte (ionic path)
connection through the metal (electronic path).

By eliminating one of these elements within a particular system, electrochemical corrosion can be halted.

### 1.5.2. Corrosive environments

According to the environment, corrosion can broadly be classified as atmospheric, soil, water, acidic, alkaline and a combination of these types. There are, however, numerous variables that constitute a particular environment. Temperature, pH value, humidity, sun exposure, concentration of corrodent, presence of microbiological organisms and numerous other factors all affect corrosive behaviour.

Regarding temperature, higher values benefit corrosion. The general rule of thumb is that corrosion rates double with each 10 ˚C increase. The increased corrosion rate results from increased activation energy for chemical and electrochemical reactions, increased diffusion rates in the electrolyte, and increased transport through the electrolyte or environment, and across films that may be formed on the metal surface.[20]

As for pH, rate of corrosion decreases at higher and increases at lower values for most metals, except for aluminium and other amphoteric metals, which tend to dissolve at higher pH.

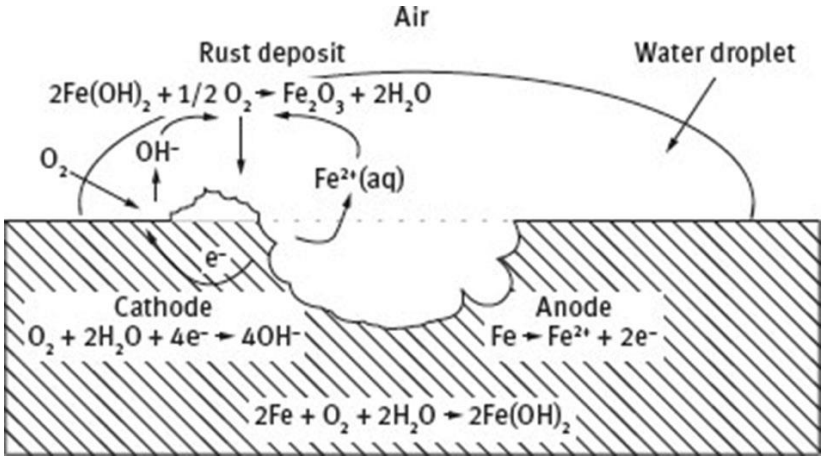


***Figure 8*** Electrochemical corrosion of iron under a droplet of water.[26]

Presence of water is crucial for electrochemical corrosion. Aqueous environments can range from very thin condensed films of moisture to bulk solutions, and will include natural environments such as the atmosphere, natural waters, soils, body fluids, etc.[22] In atmospheric and soil corrosion, humidity enables formation of thin films on the surface of the metal, which serve as an electrolyte for the corrosion process.

Thin water films also create areas with varying exposure to oxygen. The region exposed to a higher concentration of oxygen becomes a cathode, and the region exposed to lower concentrations becomes an anode, thus enabling what is known as differential oxygen corrosion (*Fig. 8*).[27]

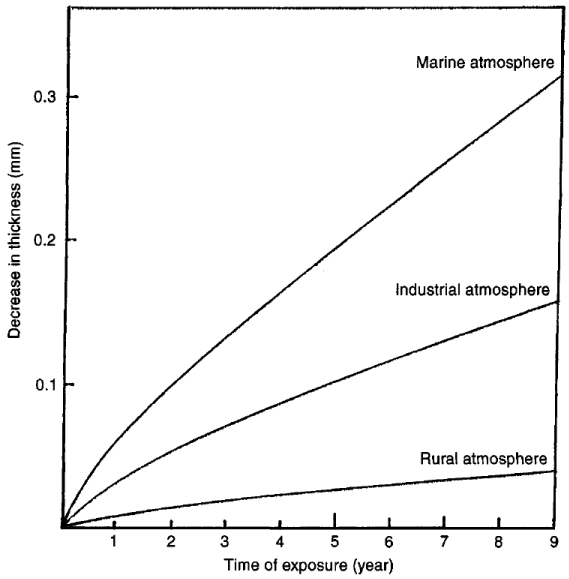


***Figure 9*** Atmospheric corrosion of steel, as a function of time in different types of atmospheres.[27]

Even though humidity plays a vital part in electrochemical corrosion, it is the pollutants that determine the rate of rusting, as in their absence rusting is not serious even in highly humid environments. For instance, as shown in *Figure 9*, corrosion product films on steel formed in relatively unpolluted environments, such as rural atmospheres, tend to be protective, resulting in a decrease in corrosion rate with time. However, in marine and industrial atmospheres, where there is a substantial presence of corrodents, such as chlorides, sulphur dioxide, various nitrogen oxides and hydrogen sulphide, the corrosion product films formed are less protective.[27]

***Table 4.*** Standard corrosion rates for metals in atmospheric conditions.[28]

| Corrosivity zones (ISO 9223) | | Typical environment | Corrosion rate for the first year of exposure (µm/year) | |
|---|---|---|---|---|
| Category | Description | | Mild steel | Zinc |
| C1 | Very low | Dry indoors | ≤1.3 | ≤0.1 |
| C2 | Low | Arid/Urban inland | >1.3 to ≤25 | >0.1 to ≤0.7 |
| C3 | Medium | Coastal or industrial | >25 to ≤50 | >0.7 to ≤2.1 |
| C4 | High | Calm sea shore | >50 to ≤80 | >2.1 to 4.2 |
| C5 | Very high | Surf sea shore | >80 to ≤200 | >4.2 to ≤8.4 |
| CX | Extreme | Ocean/Off-shore | >200 to ≤700 | >8.4 to ≤25 |

### 1.5.3. Seawater

When it comes to corrosive mediums, seawater is one of the most destructive, as it's the only natural electrolyte containing a relatively high concentration of dissolved salts. The content of dissolved salts is expressed in the terms of salinity, which for seawater averages around 35 ‰. This equates to 35 grams of salts dissolved in one litre of water. Most of the salt content falls to NaCl, around 86 wt. %, with a smaller percentage of $MgCl_2$, $MgSO_4$, $CaSO_4$, KCl, $CaCO_3$ and other inorganic salts. These are the main constituents of seawater, and they determine its salinity, as they have a higher retention time and constant concentration ratios. There are also microconstituents, organic and inorganic molecules, dissolved gasses, nutrients and trace elements, which can have an impact on corrosion in seawater.[29]

Although salinity and composition in major oceans do not deviate considerably from the average, in special areas, local conditions can modify the characteristics of seawater. For example, at places where there is a massive inlet of fresh water, e.g., from rivers or melting ice, there is a drop of salinity due to dilution. On the other hand, enclosed seas, such as the Mediterranean, Black Sea and Red Sea have a higher salinity due to higher rates of evaporation. Another example would be colder regions, where seawater usually has a higher concentration of dissolved oxygen, resulting from its increased solubility at lower temperatures. Along with dissolved salts, oxygen represents one of the most important factors in the corrosion of metals immersed in aqueous solutions.

Generally, an increase in concentration of dissolved oxygen leads to a higher corrosion rate. Oxygen also has an immense biological significance, influencing the growth of marine organisms.[22] When these organisms settle on the surface of a metal (marine fouling), deterioration of the metal may occur as a result of their metabolic activity. This is known as biological corrosion, and it is extremely pronounced in seawater environments such as tidal bays, estuaries, harbours, and coastal and open ocean seawaters, where a great variety of organisms are present. Some of these organisms are large enough to observe with the naked eye (barnacles), while others are microscopic (bacteria, algae).

Corrosion that occurs under these conditions is typically localized in its form, as organisms mostly settle individually, rather than in a continuous film. Moreover, it takes a period of months or even years before a complete cover is built up. Marine fouling can

also lead to the creation of differential oxygen cells, where the surface of the metal covered with organisms is shielded from dissolved oxygen and becomes an anode, while the exposed area acts as a cathode.[30]

Another factor that affects corrosion in seawater is fluid velocity. When it comes to stainless steels, they are more likely to be attacked in low-velocity seawater or at crevices resulting from equipment design or attachment of barnacles. Types 304 and 316 suffer deep pitting if the seawater flow rate decreases below a certain value because of the crevices produced by fouling organisms.[31] Consequently, the choice of stainless steel for seawater service depends on whether stagnant conditions can be minimized or eliminated.

## 1.6. Corrosive behaviour of stainless steels

Stainless steels, as their name implies, display an incredible resistance to corrosion in a wide range of environments and conditions. They owe their high resistance to the spontaneous formation and stability of passive chromium oxide film ($Cr_2O_3$) on their surface (*Fig. 10*).

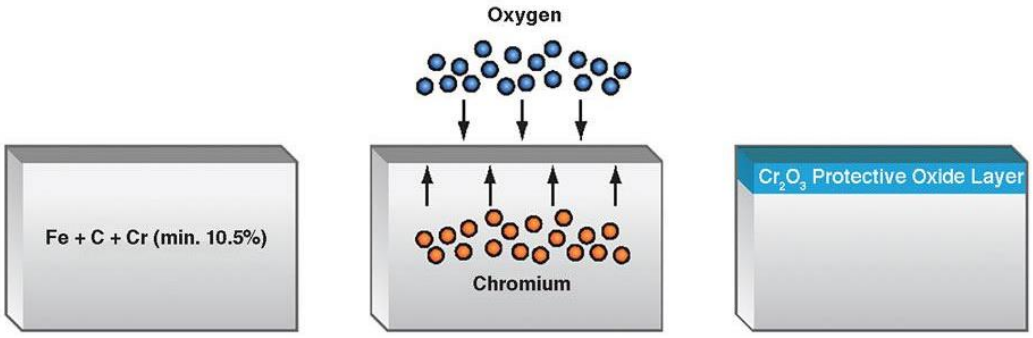


***Figure 10*** Passivation process of stainless steel.[32]

Passivity in general represents a state of low corrosion rate brought about under a high anodic driving force, or potential, by the presence of the interfacial solid film. It stands opposite to activity, in which a metal corrodes freely under an anodic driving force.[22]

The protective passive film is generated momentarily through the reaction of chromium in the alloy with an oxidizing acid or moisture and air from the environment. The actual mechanism, depicted in *Figure 10*, is very similar to the corrosion process itself, and

although the resulting oxide film is incredibly thin, around 1-10 nm, it strongly adheres to the metal surface, serving as a protective barrier against the corrosive environment.[33] Under appropriate conditions, this barrier also has the ability to regenerate through spontaneous re-passivation, in case of local damage. Therefore, passivity is not a static state, but a dynamic condition in which there is continuous dissolution and repair of the passive film on the metal surface.[34]

The minimum concentration of chromium required for passivity is a function of the type of corrosive medium, the concentration of oxygen and other corrodents, and temperature. Consequently, there is no fixed ratio of iron to chromium concentration in stainless steels that characterizes the passive state.[27]

Under atmospheric conditions, passive film forms at a Cr content of around 10.5 wt. %. However, it is relatively weak and offers limited protection. For a more complete corrosion protection a higher content of chromium is required. By raising the Cr content to 17 – 20 wt. %, which is characteristic for the AISI 300 austenitic grades, or above 25 wt. % as in duplex steels, stability of the passive film can be significantly increased.[31]

Although chromium is the main element that provides stainless steel with its corrosion resistance, a higher content of chromium can have a negative effect on mechanical properties, machinability and weldability. Thus, it is often favourable to enhance corrosion resistance for various conditions by introducing other elements to the alloy. These elements affect the capability of chromium to form and maintain a passive layer, but they individually cannot produce properties of corrosion resistance in stainless steels.[35]

The addition of aluminium to stainless steels enhances their high-temperature oxidation resistance, while niobium can be used to combine with nitrogen and carbon, reducing the possibility of intergranular corrosion. Nickel is used to stabilize austenitic structure in the AISI 200 and 300 stainless steel grades, and for increasing resistance to corrosion in reducing environments. Copper added to austenitic stainless steels provides corrosion resistance to sulfuric acid. Nitrogen increases resistance to pitting and crevice corrosion and is also used to stabilize the austenite phase. Elements like manganese, molybdenum, silicon and titanium can also be introduced in order to improve corrosion behaviour for specific conditions and to battle specific types of corrosion.[36]

Even with a high content of Cr and the addition of other beneficial elements, stainless steels are never completely resistant to corrosion. When exposed to an environment that damages, reduces, or inhibits the formation of the passive film, the corrosion resistance of the alloy becomes compromised. The presence of dirt, grease, or free iron from contact with steel tooling may interfere with the formation of a continuous passive film. Under such conditions, there is a strong possibility for corrosion to occur.[33]

Stainless steel corrosion can be described as a two-step process: initiation and propagation. If the oxide layer is unstable under given conditions, de-passivation occurs and the metal transitions from a passive to an active state. This represents the initiation of the corrosion process, while the following dissolution of the underlying metal represents propagation. De-passivation can be general or local. General de-passivation takes place across the whole surface exposed to a corrosive medium, and results in general corrosion.

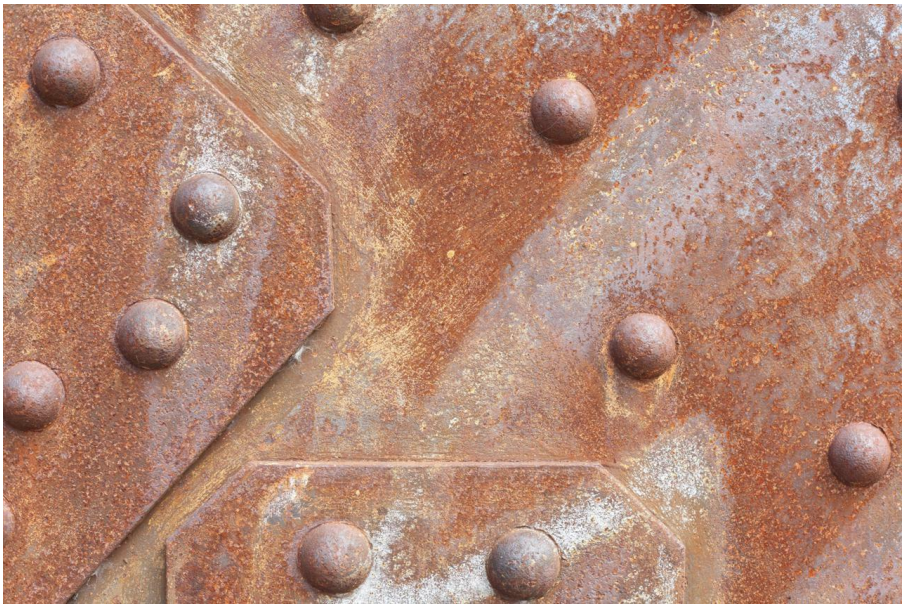

***Figure 11*** An example of general corrosion on a steel surface.[37]

General corrosion leads to a fairly uniform thinning over the exposed metal surface, and in terms of mass represents the greatest destruction of metal. However, from a technical perspective, this form of corrosion is not of too great concern, as it is easily noticeable, the lifetime of affected equipment can be accurately estimated based on relatively simple tests and usually no unexpected failures occur.[20]

For stainless steels, general corrosion occurs in reducing acids with very little oxidizing capacity, such as hydrochloric, hydroiodic or hydrobromic acid. To improve the corrosive resistance of stainless steels in these mediums, higher content of molybdenum and nickel are added.[12]

In the application of stainless steels, the occurrence of local depassivation represents the biggest danger, especially when just a negligible area of the metal becomes active. There are 4 characteristic forms of stainless-steel local corrosion:

pitting corrosion
crevice corrosion
intergranular corrosion
stress corrosion cracking.

For all of these forms of corrosion, the common characteristic is that when the passivity of the metal is lost for any reason, spontaneous re-passivation won't occur until the conditions which caused the loss in passivity have been changed. Interestingly, when the passivity of a stainless steel has been compromised, they often exhibit higher rates of local corrosion than carbon steels. This is a consequence of the cathodic to anodic surface area ratio, $S_c/S_a$. From the standpoint of the practical corrosion resistance, the least favourable ratio is a very large cathode connected to a very small anode, as more oxygen reduction or other cathodic reactions can occur, resulting in a greater corrosion current.[38]

$$I_a = i_a \cdot S_a = I_c = i_c \cdot S_c \tag{5}$$

$$i_a = i_c \cdot \frac{S_c}{S_a} \tag{6}$$

Where:
- $\boldsymbol{I_a}$ - anodic current [A]
- $\boldsymbol{i_a}$ - anodic current density [A m$^{-2}$]
- $\boldsymbol{S_a}$ - relative anodic surface area [m$^2$]
- $\boldsymbol{I_c}$ - cathodic current [A]
- $\boldsymbol{i_c}$ - cathodic current density [A m$^{-2}$]
- $\boldsymbol{S_c}$ - relative cathodic surface area [m$^2$]

Each of the four corrosion types has a different driving force, but they have a common causing factor that is crucial to the corrosion resistance of all stainless-steel grades. That common factor is the presence of halides, of which chlorides are most represented in practice. Localized adsorption of chlorides leads to an increased oxide dissolution, with subsequent thinning of the oxide film until a complete removal is achieved and active dissolution begins.[39] Especially dangerous are chloride salts that are also oxidants, such as $FeCl_3$ and $CuCl_2$.

A decrease in corrosion resistance of stainless steel can also result from sulphide precipitation caused by the presence of $SO_x$, $H_2S$, or other sulphur compounds, most commonly encountered in the oil industry. Stainless steel microstructure generally contains multiple phases which are specifically distributed in order to develop desired properties. Sulphide precipitates, however, represent undesirable inclusions which can lead to increased corrosion rates due to large electrochemical differences between the precipitate and the different alloy phases. The newly formed inclusions can either be active, partially active, noble or inert.[20,40] Active inclusions are less resistant than the surrounding matrix, and consequently dissolve. In the case of noble inclusions, which are more resistant, accelerated corrosion of the surrounding matrix can be observed. Even when the inclusion is inert, the crevices formed between the matrix and the inclusion can lead to increased corrosion. Therefore, in most cases, the presence of sulphides weakens the protective film on the stainless steel and leads to localized corrosion.[41]

Sulphides are also considered the most common cathodic poisons, as they prevent the formation of molecular hydrogen during the cathodic reaction and enhance the absorption of atomic hydrogen into the metal. This can in turn lead to hydrogen embrittlement of stainless steel and corresponding forms of corrosion.[38]

### 1.6.1. Pitting corrosion

Pitting corrosion is one of the most common and dangerous types of corrosion that affect stainless steels. It takes place in regions where the passive protective layer has been damaged, which, for stainless steels, is most often caused by the presence of halide ions, such as chlorides (*Fig. 12*). Pitting corrosion can also be initiated through non-metallic inclusions (e.g., sulphides), microscopic cracks caused by rough grinding, dust or precipitate from the surrounding medium.[35]

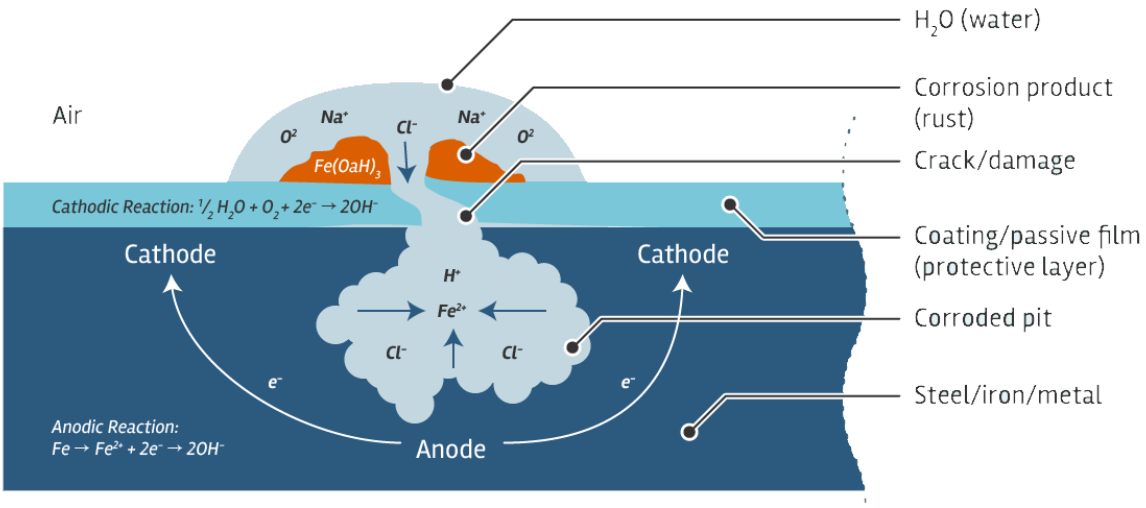


***Figure 12*** Pitting corrosion mechanism.[42]

Characteristic for this type of attack are small craters or pits which form on the surface of the affected metal. The geometrical shape of formed pits can vary substantially, as can be seen in *Figure 13*. They can be narrow and deep, wide and shallow, or they can propagate below the surface layer and form cavern-like structures.

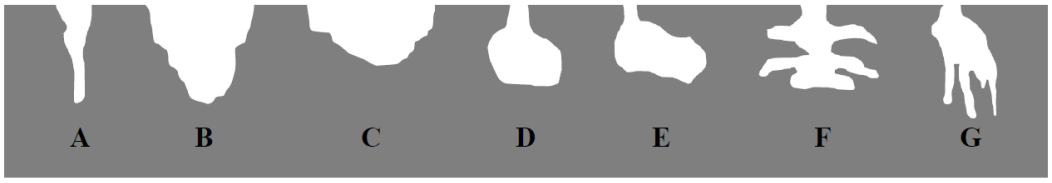


***Figure 13*** Typical shapes of corrosion pits: A) narrow, deep; B) elliptical; C) wide, shallow; D) subsurface; E) Undercutting; F) Horizontal grain attack; G) Vertical grain attack.[12]

Although the overall metal loss is minimal, it can lead to the failure of an entire construction. For example, there could be only one or two pits present on the surface of a stainless-steel tank and this slight and highly localized process could render the tank useless. Thus, the practical significance of pitting corrosion is dependent on the thickness of the metal construction and the rate of penetration.

Pitting corrosion is an auto-catalytic process. Once a pit is formed and the corrosion process begins, the aqueous medium inside the pit becomes depleted with cathodic reagents, like oxygen, while the content of metal ions ($Fe^{2+}$, $Cr^{3+}$) rises (*Fig. 12*).

The increased concentration of metal ions lowers the pH value within the pit through the process of hydrolysis and causes migration of chloride ions from the outside of the aqueous medium into the pit in order to balance the positive charges.[35] These conditions often result in an increased rate of penetration and lead to further destruction of the metal. The rate of penetration is also dependent on the number of affected areas/pits. Generally, an increase in the number of pits leads to a decrease in penetration rate, as adjacent pits have to share cathodic areas, which limits the flow of corrosion current.[24]

Since the area affected by pitting corrosion is relatively small and can be covered with corrosion products, it often goes on undetected until the metal structure is completely perforated. Consequently, these types of corrosion attacks are incredibly difficult to predict, detect and design against.

### 1.6.2. Crevice corrosion

This type of attack occurs at narrow openings or spaces between two metals or a metal and a non-metallic material. It results from an oxygen concentration difference in the electrolyte outside and inside the crevice. In the crevice, the electrolyte is devoid of oxygen, while a larger concentration is present outside of the crevice. Since oxygen is a cathodic reagent, the exterior surface serves as a cathode, while the inside becomes an anode.[20] In that instance, all 4 requirements for electrochemical corrosion are fulfilled, and a corrosion cell is formed (*Fig. 14*).

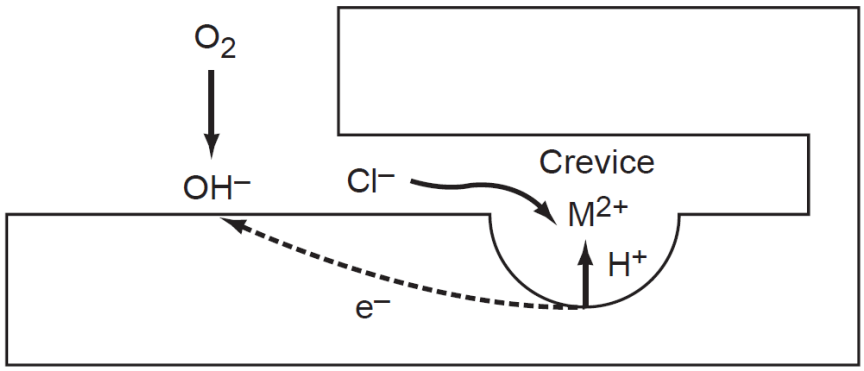


***Figure 14*** Illustration of crevice corrosion propagation mechanism.[20]

The propagation mechanism is similar to pitting corrosion. There is a dissolution of metal atoms into ions, causing a drop in pH and an increase in chloride concentration, leading to the breakdown of the passive film within the restricted space. Since a continuous presence of oxygen is needed for the formation, maintenance and regeneration of the protective oxide layer, inherent lack of oxygen within the crevice hampers re-passivation and the corrosion process can continue unimpeded.

***Figure 15*** Crevice corrosion in practice.[43]

Crevices can be created by design, or accidentally. By design, they are present in bolt holes, riveted seams, metal joints and anywhere close-fitting spaces are present (*Fig 15*). Unintentional crevices are formed in cracks, seams and other metallurgical defects. They can also be created through the deposition and accumulation of biological and non-biological materials from the environment.

There are a few ways to decrease the possibility of crevice corrosion. Mediums with a relatively high presence of chlorides should either be avoided, or grades with a higher chloride resistance should be used. For example, stainless steel grades with a higher content of Cr, Mo, N and a lower concentration of carbon, e.g., AISI 316L, have significantly better resistance to this type of attack, even when compared to other stainless-steel grades.

Cleanness is also an important factor, particularly when conditions promote deposition on metal surfaces. Regular cleaning involving mechanical methods should be commonly employed, along with filters, which remove materials that can deposit on the metal surface. Additionally, better design solutions, which avoid narrow spaces, stagnating conditions in the environment and accumulation of various deposits can also be implemented.[20]

### 1.6.3. Intergranular corrosion

What is inherent in stainless-steel grades is that they contain numerous intermetallic phases, which can have a tendency to precipitate on the grain boundaries, especially during heat treatment or welding. This process is known as sensitization, and it is a precondition for intergranular corrosion. Most notable in stainless steels is the precipitation of chromium carbide, $Cr_{23}C_6$. As a result of the precipitation of $Cr_{23}C_6$, regions adjacent to the grain boundary become depleted in chromium and start to behave as active anodes, while the interior of the grain remains passive. This frequently occurs in an aerated corrosive environment, where the smaller, chromium depleted, non-passive anode dissolves and the larger cathode reduces oxygen.[45]

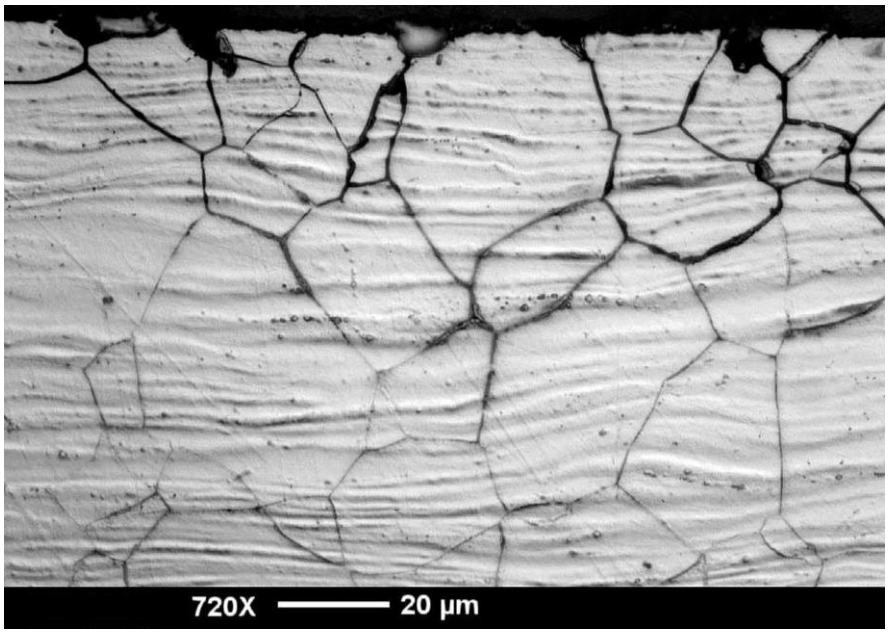


***Figure 16*** Intergranular corrosion attack in austenitic cold rolled stainless steel sheet.[44]

Intergranular corrosion starts on the surface of the metal, in the immediate vicinity of a grain boundary, but can propagate through the whole metal due to the large cathode to anode surface area ratio. The driving force is the difference in corrosion potential that develops between the grain boundary and the bulk material in adjacent grains.[45]

Although the detailed mechanism of intergranular corrosion varies with each metal alloy, for most systems, the physical appearance of the attack at the microscopic level is quite similar (*Fig. 16*). In practice, this type of corrosion bears incredible significance, as it can have intensively harmful effects on mechanical properties of a given stainless steel grade.

There are several ways to reduce the risk of intergranular corrosion. By utilizing low carbon stainless steel grades, the probability for carbide formation drops significantly. In addition, stabilizing stainless steel grades with elements such as titanium and niobium, which bind carbon from the alloy and create their own carbides, can reduce chromium carbide formation at the grain boundaries.[4]

Another way to reduce the risk of intergranular corrosion is to limit retention at temperatures at which the stainless steel becomes sensitized. For austenitic stainless steels, these temperatures typically range between 500-850 ˚C. Furthermore, heat treatment (1000-1200 ˚C) in order to dissolve chromium carbides, followed by rapid cooling, can also be used to prevent intergranular corrosion.[4]

### 1.6.4. Stress corrosion cracking

Stress corrosion cracking (SCC) can be defined as a localized occurrence of macroscopic fractures resulting from the simultaneous exposure to tensile stresses and specific environmental conditions (temperature, pressure, pH, etc.).[46] Metals and alloys subjected to these two controlling factors may develop cracks that would not occur in the absence of either. Coincidentally, movement towards higher operating stresses, derived from the more efficient use of material and more extensive use of welding as a method of fabrication led to a relatively recent increase in SCC occurrence.[27]

***Figure 17*** Stress corrosion cracking in stainless steel.[46]

Similar to previous types of corrosion, the probability for SCC in stainless steels rises with the increase in temperature and with the higher presence of $Cl^-$ and $OH^-$ ions and $H_2S$. In stainless steels, cracks can be seen to initiate at surface defects and irregularities. After initiation, cracks caused by SCC propagate either through intergranular or transgranular paths. Furthermore, there is an interplay with other types of corrosion, as corrosion pits, crevices or intergranular corrosion sites in sensitized material can provide optimal conditions for SCC initiation.[45]

The process itself is quite complicated and is brought about by cooperating effects of numerous different mechanisms, including anodic and cathodic processes, absorption, surface reactions and reactions at surface defects. Depending on the surroundings, relatively low stresses can cause SCC. Residual internal stresses generated by various production processes, such as deformation, grinding and welding can lead to this kind of destruction.[47]

SCC prevention ideally begins with the selection of an alloy which is resistant to this type of attack, preferably a ferritic or duplex stainless-steel grade, while at the same time considering other potential corrosion attacks. Modification, or rather redistribution of stress through design optimization and releasing of residual stresses after shaping and welding processes can also reduce the risk of potential attacks. The third option is to modify the environment, either by removing aggressive pollutants (chlorides, sulphides) or by introducing corrosion inhibitors.[27]

# 2. EXPERIMENTAL PART

## 2.1. Materials and methods

Investigations were performed on the AISI 304L and AISI 316L stainless steels, whose chemical compositions are listed in *Table 5.*

***Table 5*** Chemical composition of investigated stainless steels.

| Sample | Content of alloying elements / wt. % | | | | | | | |
|---|---|---|---|---|---|---|---|---|
| | Cr | Ni | Mn | Mo | Si | Cu | C | Fe |
| AISI 304L | 16.76 | 8.66 | 2.23 | 0.11 | 0.52 | 0.38 | 0.03 | 71.58 |
| AISI 316L | 16.47 | 10.54 | 1.16 | 2.53 | 0.47 | 0.27 | 0.002 | 68.55 |

Test samples of stainless steel purchased from commercial sources (Ronsco, China) were received in the form of a cylinder rod with a diameter of 6 mm and 150 mm in length. Samples for making the electrodes for the electrochemical measurements were obtained by cutting the steel rods with a metallographic cutting machine, at the length of 20 mm. Electrical contact was achieved by soldering the Cu wire on the base of the cylinder, or by drilling a hole on one side of the cylinder, then threading the drilled hole with M3 threads and inserting a copper M3 threaded rod.

The specimens were mounted into cold-curing acrylic resin, with only the opposite cylinder base staying uncovered, serving as the working surface of the electrode. In order to remove surface impurities and irregularities, and to enable uniform surface conditions, the stainless-steel samples were gradually sanded with different grain fineness (sandpapers marked P180, P400, P800, P1200, and P2500) and polished with the diamond paste with a particle size 0.5 μm. After polishing, the samples were additionally cleaned and degreased in an ultrasonic bath in 70 % ethanol, and after that, in deionized water (10 min). Investigations were performed in seawater collected at the beach Žnjan in Split. The characteristics of the used seawater are listed in *Table 6.*

***Table 6*** Characteristics of seawater used in the experiments.

| Medium | pH | Conductivity/ mS $cm^{-1}$ |
|---|---|---|
| Seawater | 8.10 | 57.7 |

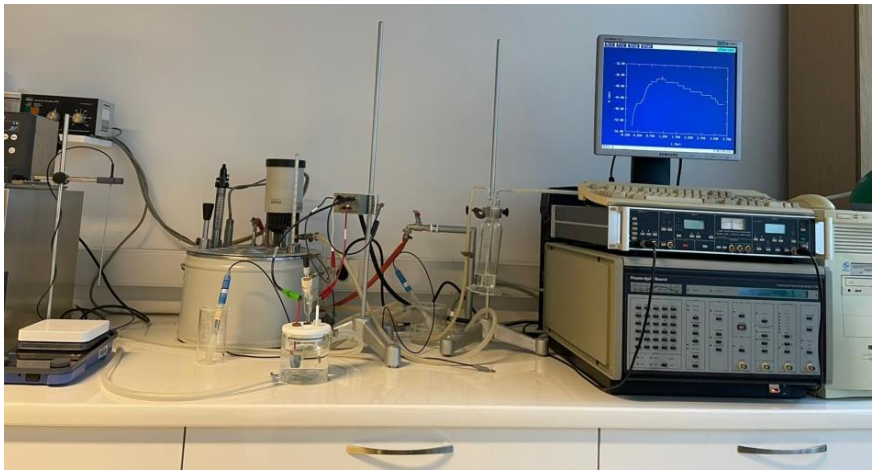

***Figure 18*** Electrochemical measurement equipment setup.

Seawater solutions containing sulphide ions were prepared by, firstly, calculating the needed mass of p.a. pure $Na_2S$ x $3H_2O$ salt. In order to prepare 1 L of seawater solution with a $S^{2-}$ concentration of 40 ppm, 164.797 mg of the salt was needed. Next, the calculated mass of salt was weighed on an analytical scale, after which it was dissolved in 1 L of seawater. The 10-ppm solution was prepared by diluting 0.125 L of 40 ppm solution in a 0.5 L volumetric flask.

The apparatus used for the electrochemical measurements is shown in *Figure 18*.

Electrochemical measurements were performed with the EG&G Princeton Applied Research model 273A potentiostat-galvanostat, connected with the 200 ml double wall glass cell, equipped with the working electrode, Ag/AgCl as reference electrode and Pt-sheet counter-electrode. Glass cell was connected to the cooling bath thermostat Huber Kiss K6 with the flexible silicone hose to maintain the desired operating temperatures (15, 25 and 35 °C). A closer look at the 3-electrode electrochemical cell is shown in *Figure 19*.

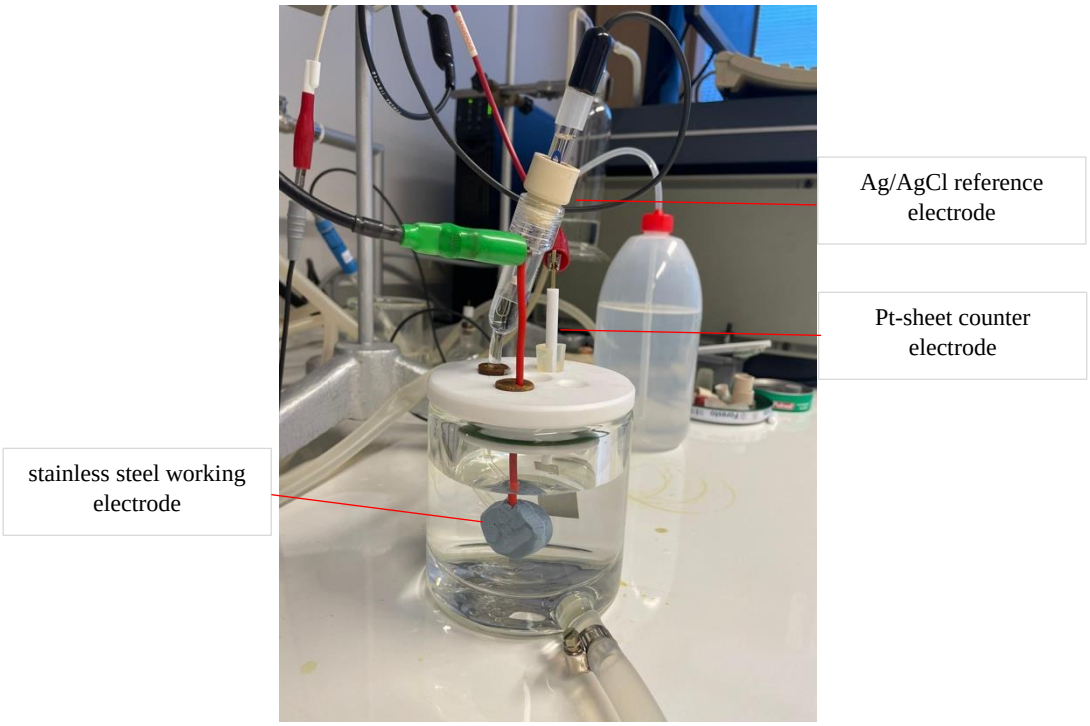


***Figure 19*** Double wall electrochemical cell with electrodes.

The open circuit potential ($E_{OC}$) was recorded every 20 seconds after immersing the working electrode in the electrolyte for a period of 60 minutes.

Linear polarization measurements were recorded in a potential range ± 20 mV vs. $E_{OC}$ with a scan rate of 0.2 $mVs^{-1}$.

Potentiodynamic polarization measurements were performed at a scan rate of 1 $mVs^{-1}$ starting from -250 mV vs. $E_{OC}$ to 800 mV.

***Figure 20*** Light microscope MXFMS-BD Ningbo Sunny Instruments co.[48]

For the electrode surface examination after the electrochemical measurements, a light microscope MXFMS-BD, Ningbo Sunny Instruments co. was used (*Fig. 20*).

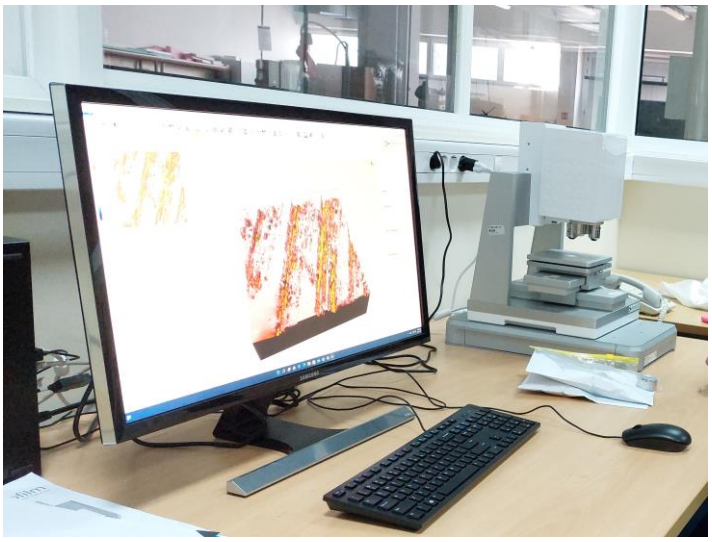

***Figure 21*** Profilm3D 3D optical profilometer.

The depth of pitting corrosion was examined using the Profilm3D 3D optical profilometer (KLA Corporation, Milpitas, CA, USA) (*Fig. 21*)

# 3. RESULTS

## 3.1. Results of the open circuit measurements

The results for the open circuit measurements of AISI 304L and AISI 316L stainless steels exposed to seawater for 60 minutes at different temperatures are shown in *Figures 22* and *23*.

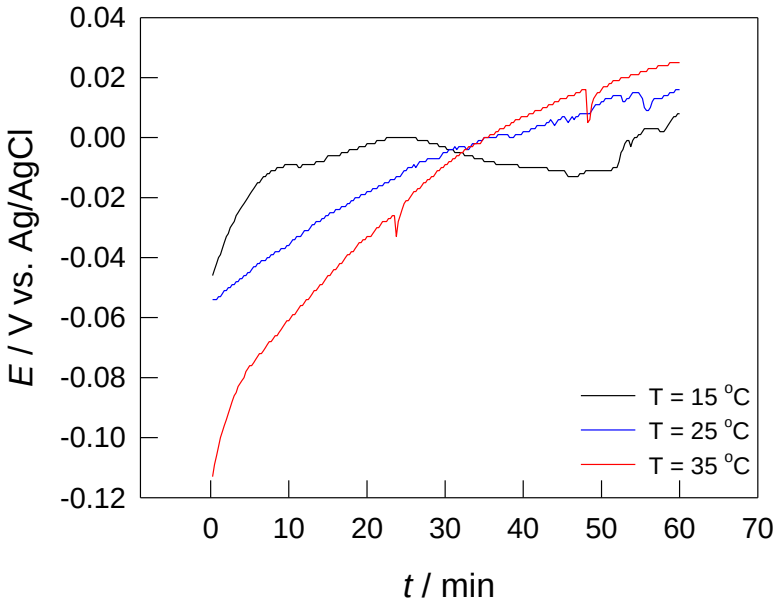


***Figure 22*** Open circuit potential curves for AISI 304L stainless steel in seawater at different temperatures.

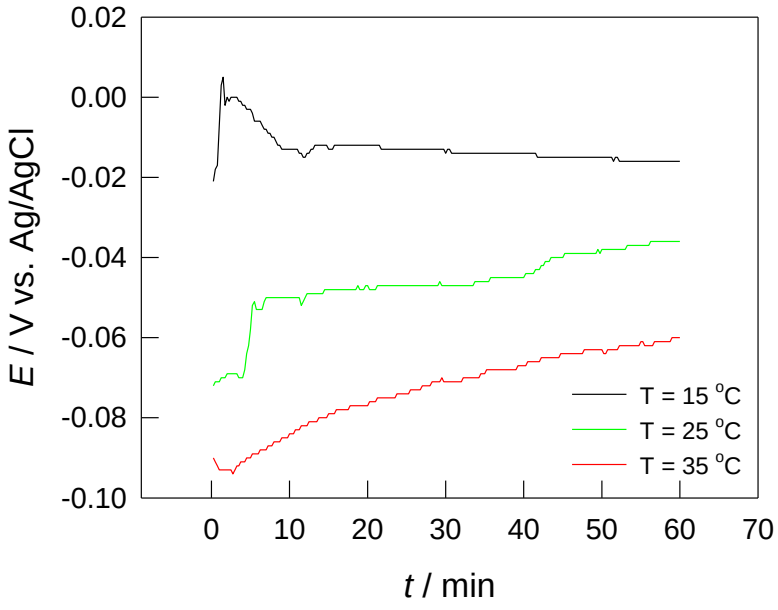


***Figure 23*** Open circuit potential curves for AISI 316L stainless steel in seawater at different temperatures.

The results for the open circuit measurements of AISI 304L and AISI 316L stainless steels exposed to seawater for 60 minutes and polluted with 10 and 40 ppm of $S^{2-}$ at 25 ℃ are shown in *Figures 24* and *25*.

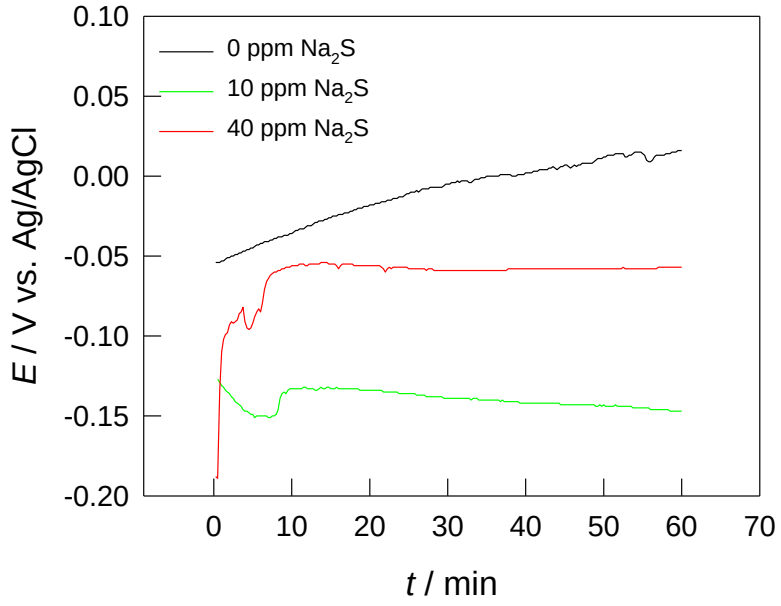


***Figure 24*** Open circuit potential curves for AISI 304L stainless steel in seawater polluted with the 10 and 40 ppm of $S^{2-}$ at $T$ = 25℃.

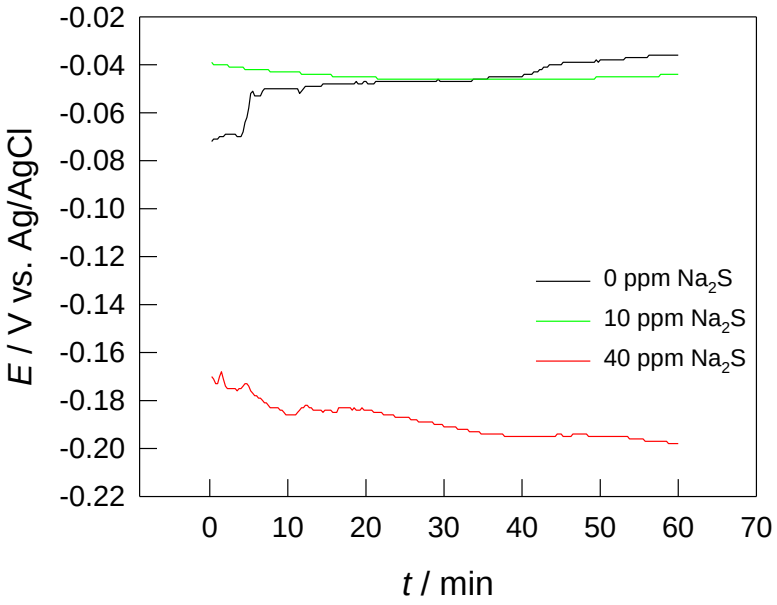


***Figure 25*** Open circuit potential curves for AISI 316L stainless steel in seawater polluted with 10 and 40 ppm of $S^{2-}$ at $T$ = 25℃.

## 3.2. Results of the linear polarization measurements

The results for the linear polarization measurements in the vicinity of $E_{corr}$ are shown in *Figures 26-29.*

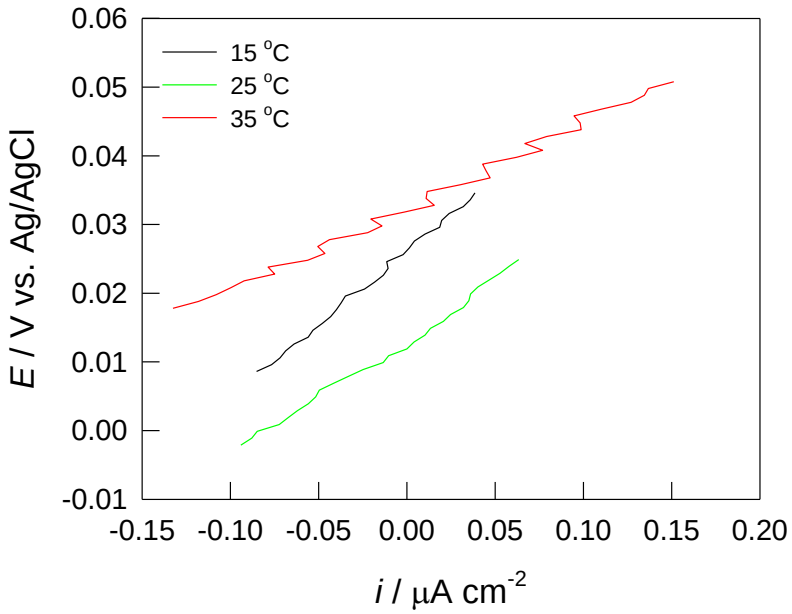


***Figure 26*** Linear polarization curves for AISI 304L in seawater at different temperatures.

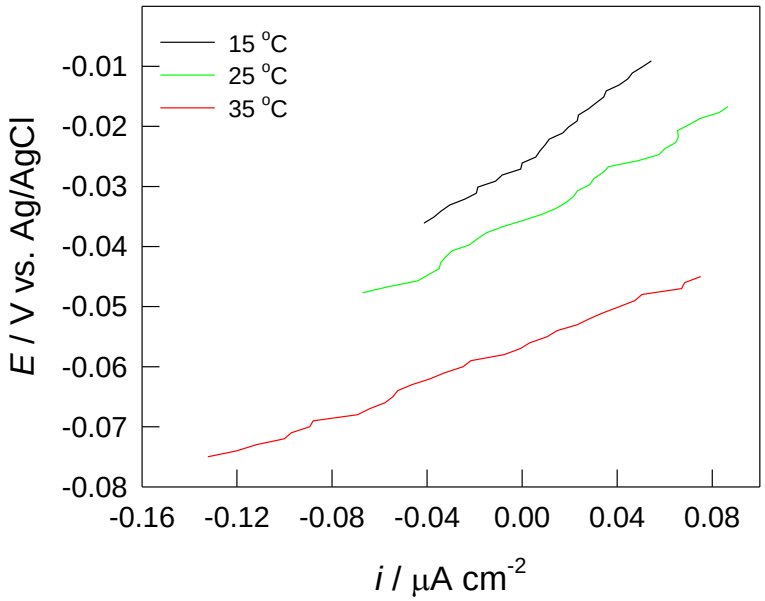


***Figure 27*** Linear polarization curves for AISI 316L in seawater at different temperatures.

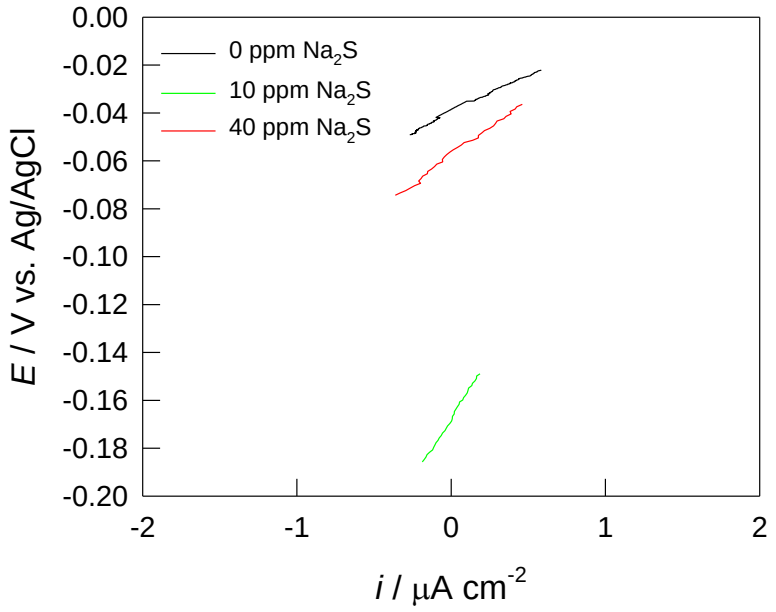


***Figure 28*** Linear polarization curves for AISI 304L in seawater polluted with 10 and 40 ppm of $S^{2-}$ at 25°C.

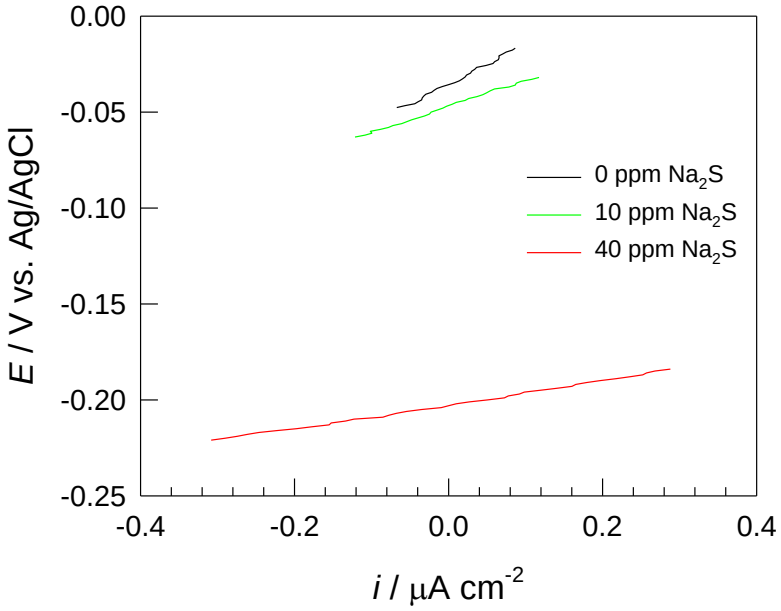


***Figure 29*** Linear polarization curves for AISI 316L in seawater polluted with 10 and 40 ppm of $S^{2-}$ at 25°C.

## 3.3. Results of the potentiodynamic polarization measurements

Potentiodynamic polarization measurements are chosen as the last electrochemical method for the corrosion investigations of AISI 304L and AISI 316L stainless steels due to its surface destructivity, as the measurements are performed in a wide potential area. The results of these measurements are presented in *Figures 30-33*.

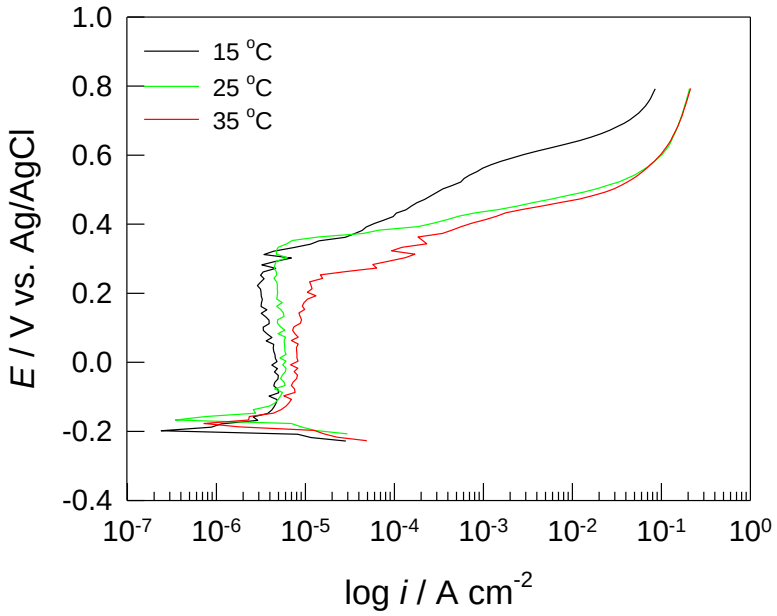


***Figure 30*** Potentiodynamic polarization curves for AISI 304L in seawater at different temperatures.

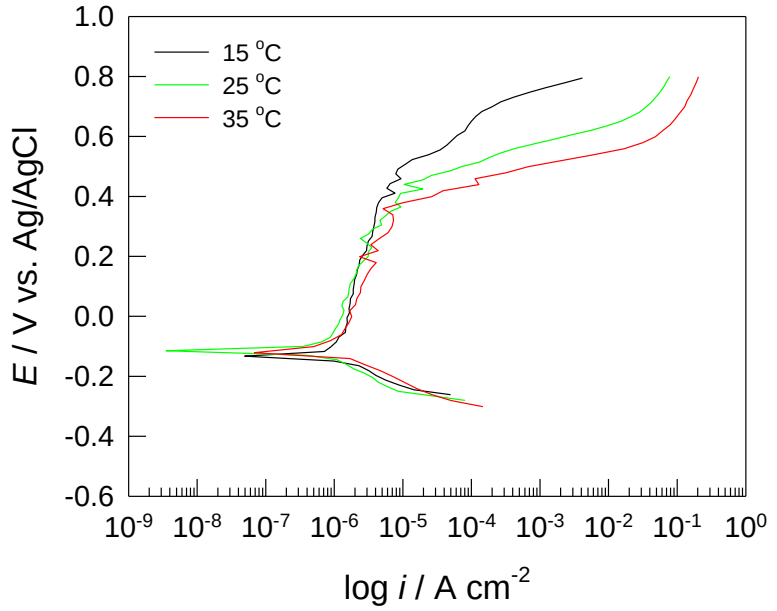


***Figure 31*** Potentiodynamic polarization curves for AISI 316L in seawater at different temperatures.

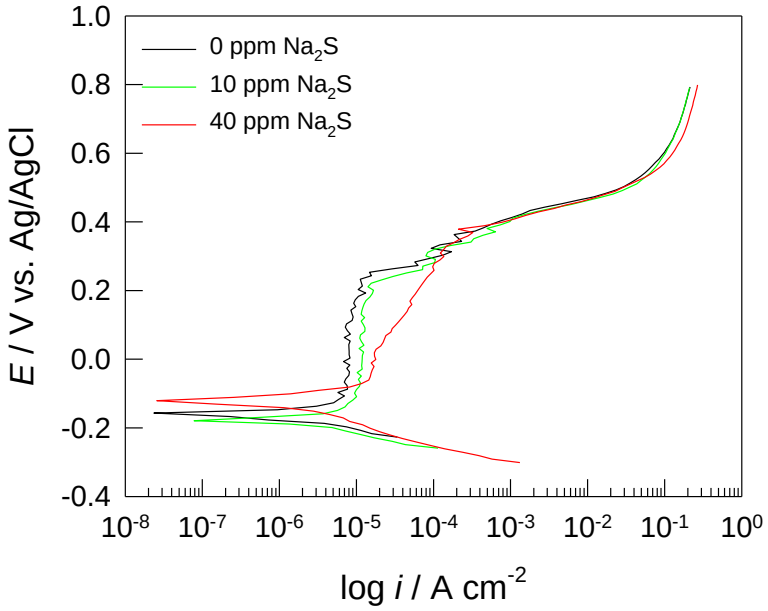


***Figure 32*** The influence of $S^{2-}$ concentration on potentiodynamic polarization curves for AISI 304L in seawater at 25°C.

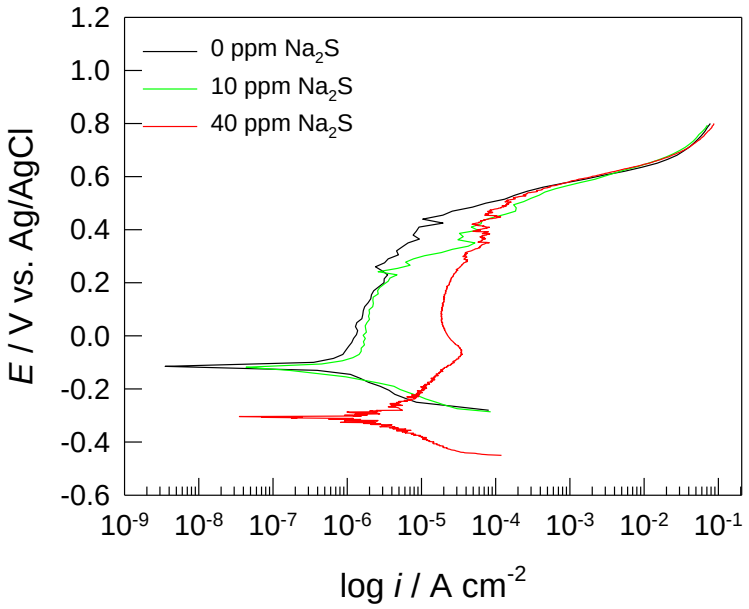


***Figure 33*** Potentiodynamic polarization curves for AISI 316L in seawater polluted with 10 and 40 ppm of $S^{2-}$ at 25°C.

## 3.4. Results of the electrode surfaces analysis by optical microscope

After the electrochemical measurements, electrode surfaces were investigated with the optical microscope, with the results shown in *Figures 34-41*.

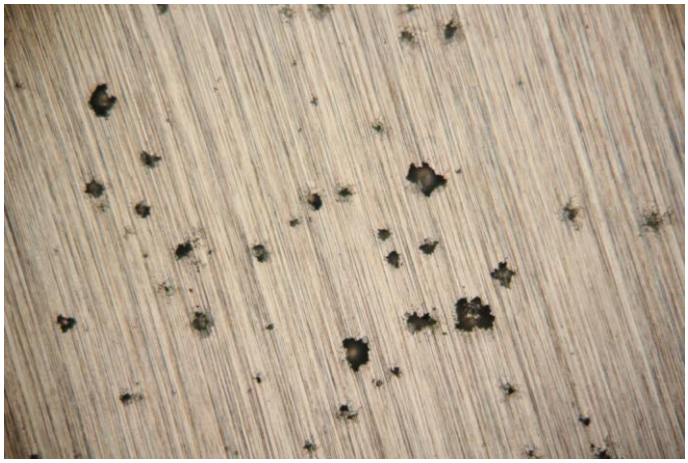

***Figure 34*** Optical micrographs for the AISI 304L after potentiodynamic polarization measurements in seawater at 15℃ (magnification 100 times).

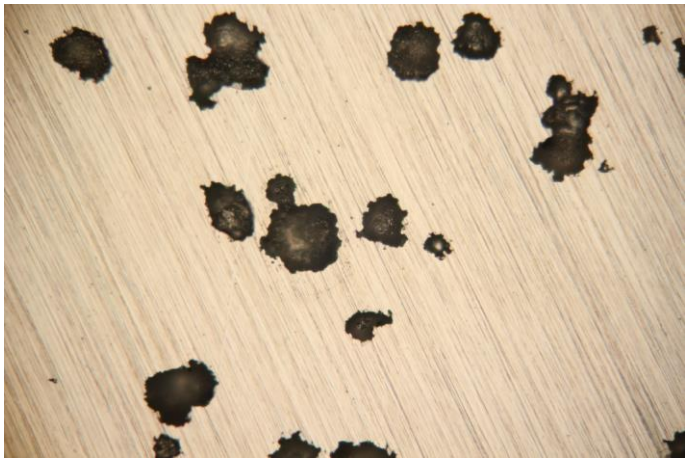

***Figure 35*** Optical micrographs for the AISI 304L after potentiodynamic polarization measurements in seawater at 25℃ (magnification 100 times).

***Figure 36*** Optical micrographs for the AISI 304L after potentiodynamic polarization measurements in seawater at 35℃ (magnification 100 times).

***Figure 37*** Optical micrographs for the AISI 316L after potentiodynamic polarization measurements in seawater at 15℃ (magnification 100 times).

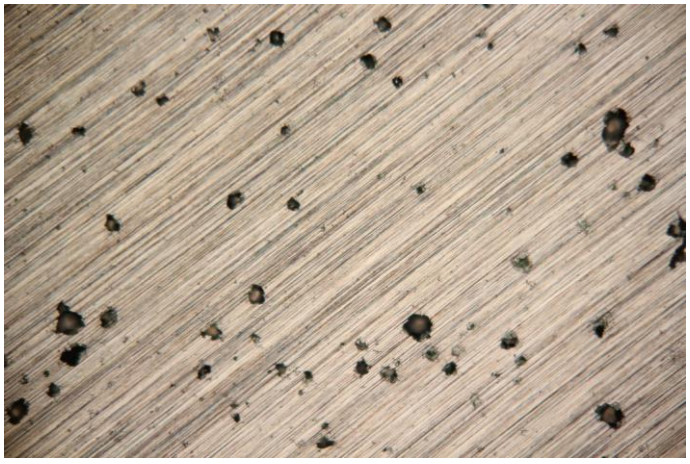

***Figure 38*** Optical micrographs for the AISI 316L after potentiodynamic polarization measurements in seawater at 25℃ (magnification 100 times).

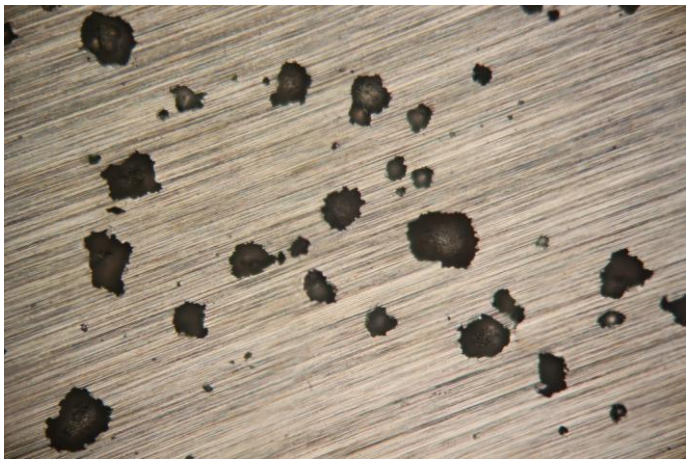

***Figure 39*** Optical micrographs for the AISI 316L after potentiodynamic polarization measurements in seawater at 35℃ (magnification 100 times).

***Figure 40*** Optical micrographs for the AISI 304L after potentiodynamic polarization measurements in seawater in the presence of 10 ppm of $S^{2-}$ at 25℃ (magnification 100 times).

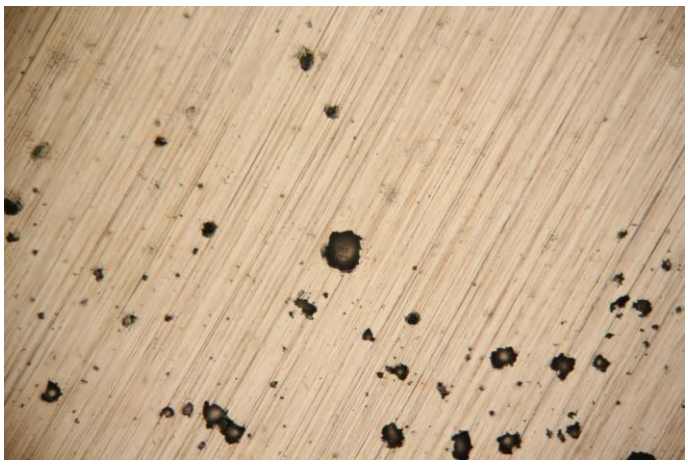

***Figure 41*** Optical micrographs for the AISI 316L after potentiodynamic polarization measurements in seawater in the presence of 10 ppm of $S^{2-}$ at 25℃ (magnification 100 times).

## 3.5. Results of the 3D optical profiling surface measurement

After the electrochemical measurements, 3D optical profiling surface measurements were performed with Profilm3D 3D optical profilometer in order to investigate the width and depth of the pits. The influences of the temperature of seawater and $S^{2-}$ on the width and depth of the pits are presented in *Figures 42-44* for the AISI 316L, and *45-47* for the AISI 304L.

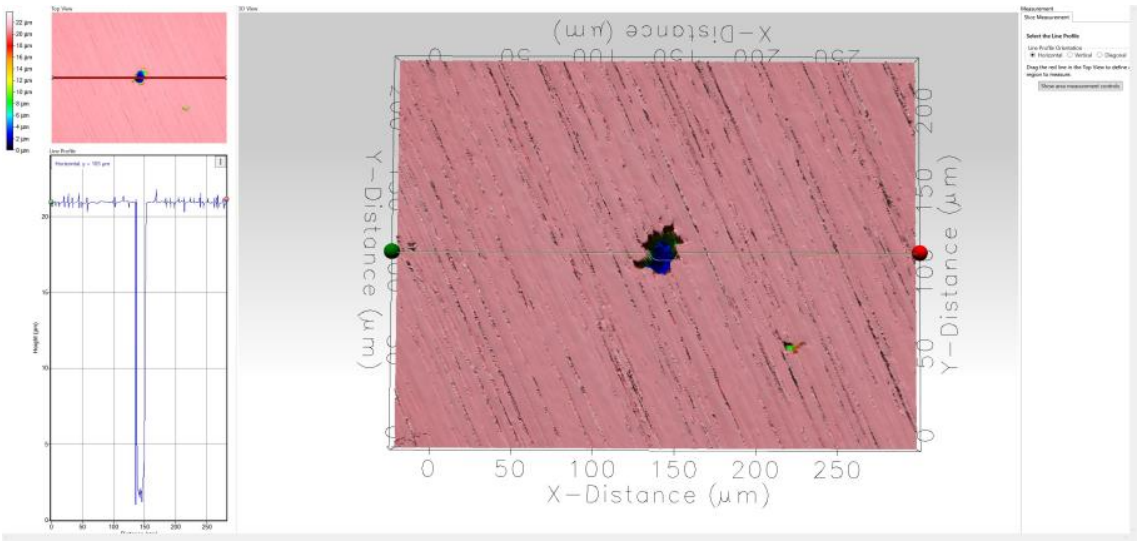


***Figure 42*** Topographical view of the segment of the corroded AISI 316L surface after potentiodynamic polarization method in seawater at 15°C.

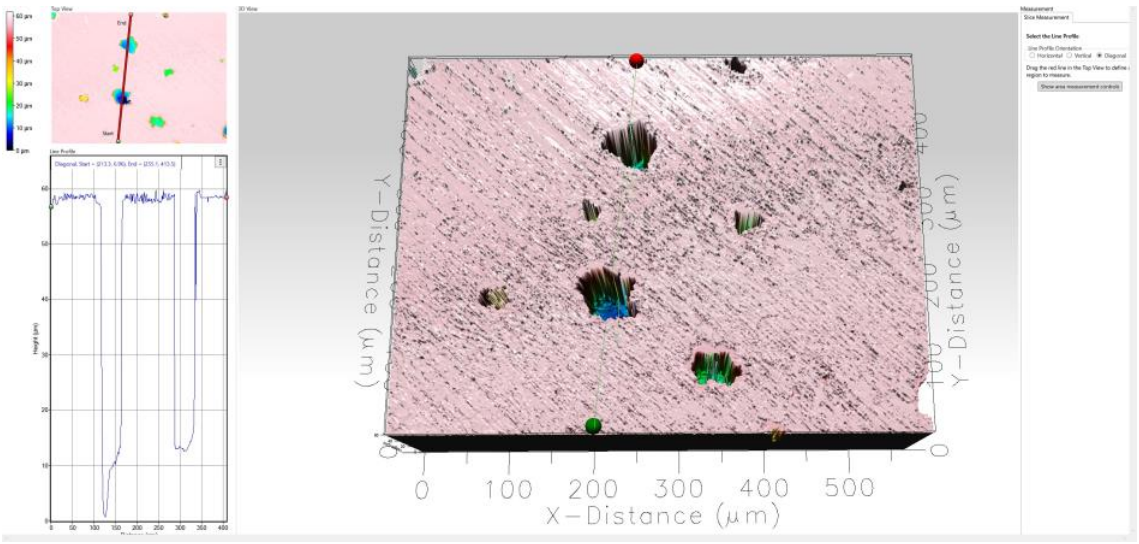


***Figure 43*** Topographical view of the segment of the corroded AISI 316L surface after potentiodynamic polarization method in seawater at 25°C.

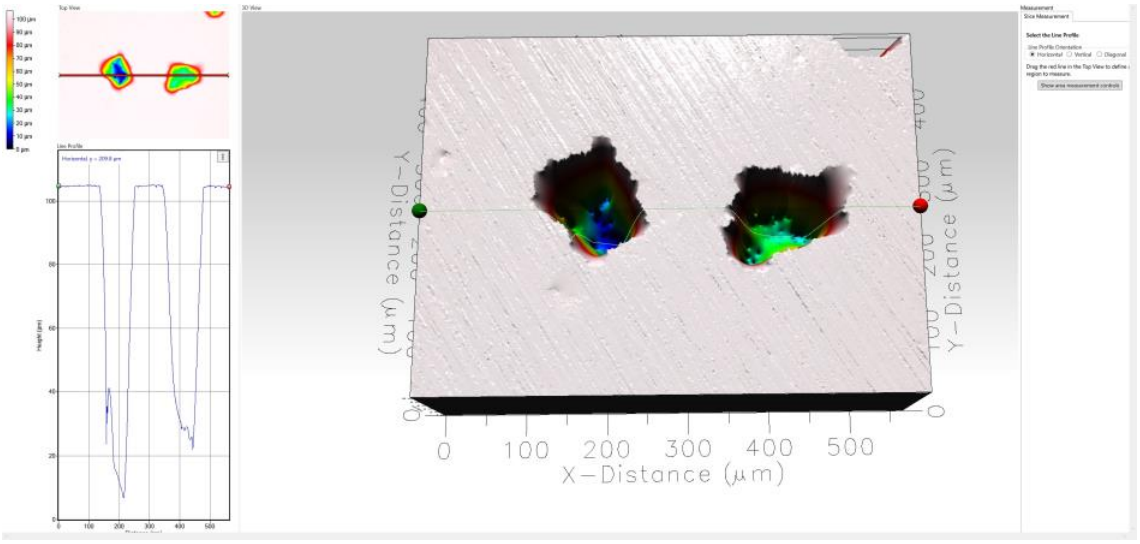


***Figure 44*** Topographical view of the segment of the corroded AISI 316L surface after potentiodynamic polarization method in seawater at 35℃.

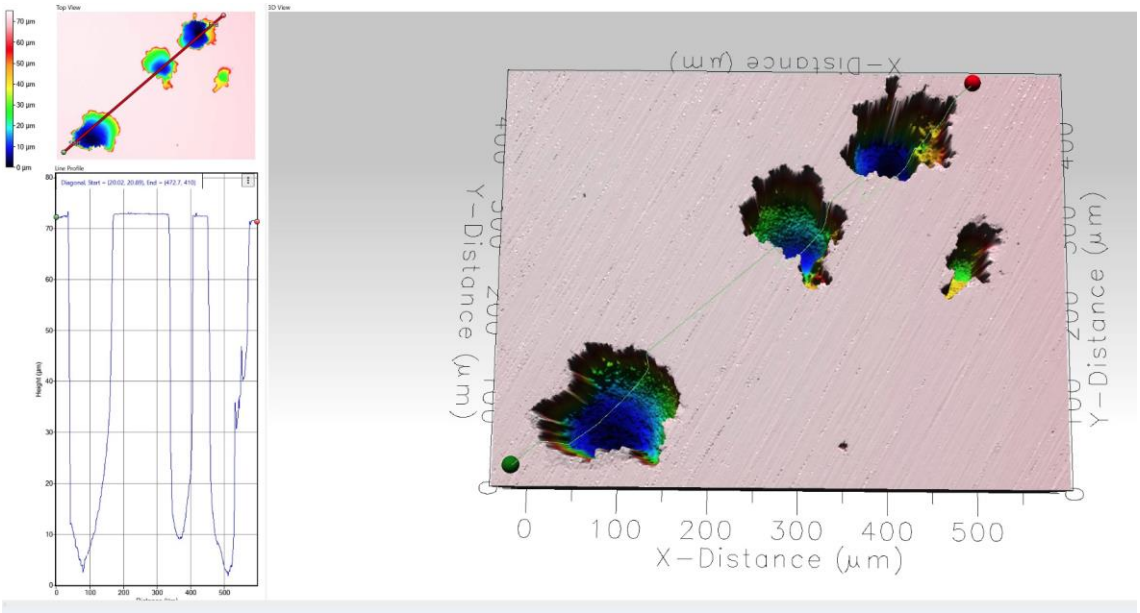


***Figure 45*** Topographical view of the segment of the corroded AISI 304L surface after potentiodynamic polarization method in seawater at 25℃.

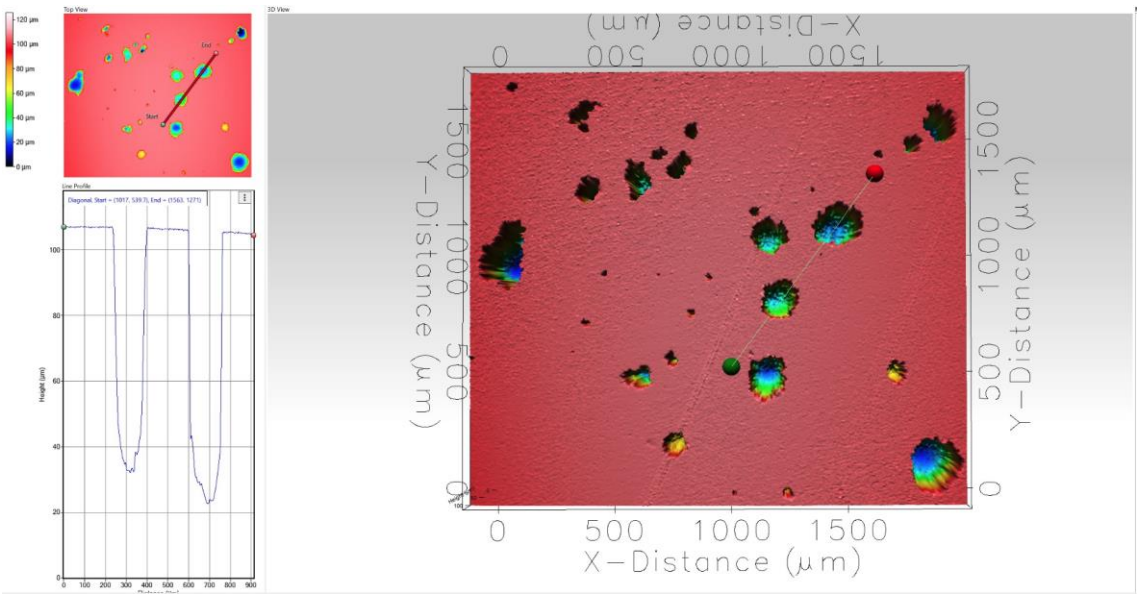


***Figure 46*** Topographical view of the segment of the corroded AISI 304L surface after potentiodynamic polarization method in seawater polluted with 10 ppm of $S^{2-}$ at 25°C.

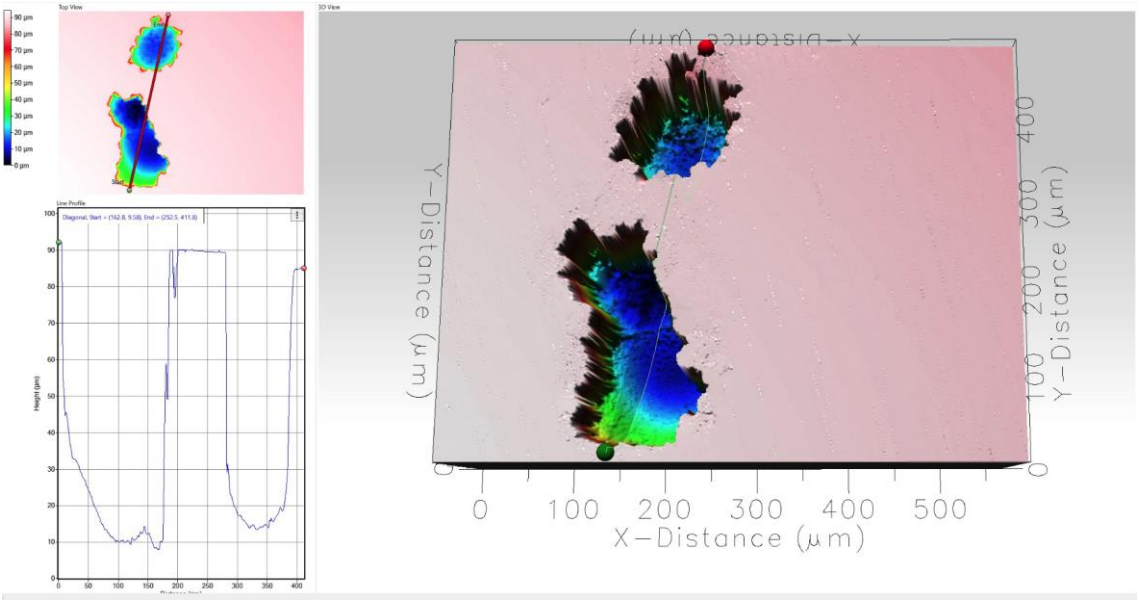


***Figure 47*** Topographical view of the segment of the corroded AISI 304L surface after potentiodynamic polarization method in seawater polluted with 40 ppm of $S^{2-}$ at 25°C.

# 4. DISCUSSION

Besides the intensive impact of chlorides and other halide ions naturally present in seawater, pollutants can also have a high influence on the corrosion of metals. Today, there is a deep global concern about the influence of pollutants on the environment, including soil, air and in particular water, and about their effect on the durability of engineering materials and the deterioration of structures and infrastructure. Human and industrial activities increase the generation of $CO_2$, $H_2S$ and $NH_3$. Dissolved-free sulphide has been proven to be a very aggressive species towards many different metals and alloys, including different types of steel, copper and copper alloys.[49-52] However, results proving the opposite have also been published, in which sulphide provided strong corrosion inhibition under specific conditions due to the formation of the protective iron sulphide layers.[53]

*Figures 22* and *23* show the open circuit curves for AISI 304L and AISI 316L stainless steels exposed to seawater for 60 minutes at different temperatures. The values of $E_{OC}$ change in the positive direction with time, which is a little more pronounced for the AISI 304L stainless steel. For the AISI 316L stainless steel (*Fig. 23*), after an initial increase in $E_{OC}$ in the first five minutes of measurements, a small decline in $E_{OC}$ values is observed for the measurement at the 15°C, after which the potential exhibits a constant value till the end of the measurement. For the measurement at 25°C, after approximately 5 minutes of increase, the potential becomes relatively stable with a small inclination towards positive values. A constant increase of $E_{OC}$ is observed for the measurement at 35°C, but the starting $E_{OC}$ exhibits the most negative value. It is interesting to note that the increase in electrolyte temperature leads to larger changes in the open circuit potential for both investigated steels. *Figure 24* shows the open circuit potential curves for the AISI 304L stainless steel exposed to the unpolluted and polluted seawater with the $S^{2-}$, in the concentration of 10 and 40 ppm, at 25°C. The presence of $S^{2-}$ ions in the solution led to some changes in $E_{OC}$ curves. The highest changes are observed at the beginning of the measurements. For both concentrations of $S^{2-}$ ions, a stable potential value is reached after 10 minutes, and it remains almost constant until the end of the measurement. In the case of AISI 316L stainless steel (*Fig. 25*), a slowly decreasing potential value with time is observed for both $S^{2-}$ ion concentrations. The more significant changes in the potential values at the beginning of the measurements are present because a certain time is required to reach stable conditions in the electrochemical cell after the measurement has started.[54] Linear polarization measurements were the second electrochemical method applied in this analysis, immediately after measuring the open circuit potential. As the potential

perturbation in this method is very small (only ±20 mV around $E_{OC}$), linear polarization is essentially a non-destructive method, which is the main advantage over other DC corrosion measurement methods.[55,56]

The slope of a line is the change in its Y values divided by the change in its X values, e.g., the change in potential divided by the corresponding change in current density. This relationship can be expressed by *Equation 7*:

$$Slope = \frac{\Delta E}{\Delta i} = R_p\ (\Omega\ cm^2) \tag{7}$$

Thus, the slope expressed in Ω $cm^2$ is referred to as corrosion or polarization resistance.[55,56]

The results of the linear polarization measurements were shown in *Figures 26-29*. The slopes of the lines are decreasing for both AISI 304L and AISI 316L stainless steel with the increase in seawater temperature (*Fig. 26* and *27*) indicating the negative effect of the rising temperature on the corrosion resistance of the investigated materials.

A decrease in corrosion resistance is also observed in the measurements in seawater polluted with $S^{2-}$ ions. In this case, the lowering of the slope is more pronounced in the presence of the higher concentration of $S^{2-}$ ions, indicating its negative effect on the corrosion stability of investigated stainless steels. Values of $R_p$, determined from the slopes of the lines, are presented in *Table 7*.

***Table 7*** Polarization resistance values for AISI 304L and AISI 316L in seawater without and in the presence of different concentrations of sulphide.

| | Temperature of clean seawater | | | $S^{2-}$ concentration | |
|---|---|---|---|---|---|
| Material | 15°C $R_p$ (kΩ $cm^2$) | 25°C $R_p$ (kΩ $cm^2$) | 35°C $R_p$ (kΩ $cm^2$) | 10 ppm $R_p$ (kΩ $cm^2$) | 40 ppm $R_p$ (kΩ $cm^2$) |
| AISI 304L | 212.789 | 167.150 | 116.050 | 101.990 | 46.375 |
| AISI 316L | 284.241 | 209.320 | 149.820 | 145.842 | 62.642 |

The potentiodynamic polarization method was used as a final electrochemical method for the analysis of corrosion resistance of AISI 304L and AISI 316L stainless steel in fresh seawater at different temperatures, as well as in seawater polluted with $S^{2-}$ ions at 25°C. The results were presented in *Figures 30-33*.

*Figure 30* shows potentiodynamic polarization curves for AISI 304L in seawater at different temperatures. The main differences between curves can be observed in the anodic region. Namely, the width of the passive region decreases with increasing

temperature, which is especially pronounced at the temperature of 35℃. In addition, the values of passive current density reach the lowest point for the measurements at the temperature of 15℃, while exhibiting an increase in value with the increasing temperature. A similar case is observed for the measurements with AISI 316L (*Fig. 31*). Moreover, a significant increase of anodic current density is observed above 0.55 V for the measurement at 15℃, 0.5 V for the measurement at 25℃, and 0.4 V for the measurement at 35℃, indicating the rupture of the surface oxide film and the evolution of pitting corrosion.

AISI 316L shows similar behaviour in seawater, where the breakdown potentials of the oxide film have a slightly more positive value compared to AISI 304L steel (*Fig. 32*). Potentiodynamic polarization curves obtained in seawater polluted with sulphide are shown in *Figure 33* for the AISI 304L and in *Figure 34* for AISI 316L stainless steel. The substantial differences in the behaviour of stainless-steel samples are visible in the passive domain of the polarization curves. The passive anodic current becomes higher in the presence of $S^{2-}$ ions and is also deformed for the measurements in the highest concentration of $S^{2-}$ ions (*Fig. 33* and *34*).

*Table 8* shows the corrosion parameters for the AISI 304L and 316L stainless steels in seawater solution at different temperatures, without and in the presence of different concentrations of sulphide ions at 25℃, obtained from the potentiodynamic polarization measurements.

***Table 8*** Corrosion parameters obtained from potentiodynamic polarization measurements

| | AISI 304L | | AISI 316L | |
|---|---|---|---|---|
| | $i_{corr}$ (μA $cm^{-2}$) | $E_{corr}$ (V) | $i_{corr}$ (μA $cm^{-2}$) | $E_{corr}$ (V) |
| 15 ℃ | 1.89 | -0.176 | 0.95 | -0.133 |
| 25 ℃ | 2.56 | -0.173 | 1.26 | -0.083 |
| 35 ℃ | 3.36 | -0.153 | 1.86 | -0.107 |
| 10 ppm $S^{2-}$ | 3.95 | -0.190 | 1.70 | -0.095 |
| 40 ppm $S^{2-}$ | 5.85 | -0.110 | 3.20 | -0.195 |

From *Table 8*, it is evident that an increase in temperature leads to an increase in values of corrosion current densities. A similar effect is observed with the increase in sulphide concentration in seawater.

After every potentiodynamic polarization measurement, the electrode was removed from the electrochemical cell, and then thoroughly washed in deionized water in an ultrasonic bath. The goal of this treatment of the electrodes was to remove any accumulations of corrosion products on the surface of the electrodes, as well as in pits caused by pitting corrosion. After the treatment, electrodes were dried with circulating hot air and then investigated with the light microscope in the bright field at 100 times magnification. The results are shown in *Figures 34-41*.

The pits on the electrode surfaces of both types of stainless steels are clearly visible in these figures. It is also obvious that the size of the pits increased with the temperature of the seawater. It should be noted that the bigger pits are observed for the AISI 304L steel for the same seawater temperature, which confirmed that the AISI 304L stainless steel is more prone to corrosion compared to AISI 316L steel. Pits have irregular shapes, which is the consequence of their mutual joining due to the more intense corrosion at higher temperatures. The introduction of the sulphide ions in seawater solution leads to variations in the shape of the pits and their size, which becomes bigger for the AISI 304L stainless steel (*Fig. 40*), while for the AISI 316L the number of pits on the alloy surface increased (*Fig. 41*).

More detailed information about the size of the pits and their depth was obtained using profilometry measurements. The technique of the 3D non-contact profilometer analysis provides an ideal, user-friendly capability to maximize surface studies when pitting analysis is needed; along with the benefits of combined 2D and 3D capability.[58]

The influence of the temperature of seawater on the width and depth of the pits is presented in *Figures 42-45* for the AISI 316L stainless steel. From *Figure 42* for the potentiodynamic polarization in fresh seawater at 15℃, minimal surface damages are observed. The scanned pit has a diameter of approximately 25 μm and a depth of approximately 20 μm. The situation on the AISI 316L surface after potentiodynamic polarization measurement at 25℃ is much worse than at 15℃, which can be seen in *Figure 43*. Many small pits are visible on the surface, indicating intensive pitting corrosion. Line analysis performed across the surface (top left corner) has shown an increase in the width and depth of the pit. Analysed pits have a depth between 50 and 60 microns and width of around 50 microns.

The worst situation is observed during the analysis of AISI 316L surface after potentiodynamic polarization at 35℃, with 2 intensive pits in the focus (*Fig. 44*). Line

analyses have shown that their depth is around 80-100 µm and their width around 100-125 microns.

A similar trend was observed for the measurements with AISI 304L samples at different seawater temperatures, but the situation was slightly worse compared to 316L. *Figure 45* shows a segment of the AISI 304L surface after potentiodynamic polarization at 25°C. Line analysis of the 3 pits depicted on the surface revealed that the diameter of the pits extended to 80-120 µm, and their depth reached around 70 µm, which indicates a more severe pitting attack than in the case of AISI 316L at the same conditions.

Finally, in *Figure 46* and *Figure 47*, the analysis of pitting damages on the AISI 304L steel surfaces after potentiodynamic polarization method in polluted seawater with 10 ppm and 40 ppm of $S^{2-}$ ions have been shown. The presence of sulphide leads to the evolution of pits, with depth of around 90 µm and diameter up to 150 µm.

The worsening corrosion properties of the stainless steels exposed to the polluted seawater can be explained by the adsorption of the $S^{2-}$ ions on the surface, disturbing the growth of the oxide layer and decreasing its effectiveness. In this way, the formation of sulphur-containing phases in the outermost layer of the oxide film is observed.[50,57] At the higher sulphide concentration, local acidification is efficient enough so that the primary passive film is dissolved, and active dissolution of the metal mediated by sulphide occurs, according to the following equations:[59]

$$M + HS^- \rightarrow MHS_{ad} + e^- \quad (8)$$

$$MHS_{ad} \rightarrow MHS^+_{ads} + e^- \quad (9)$$

$$MHS^+_{ads} \rightarrow M^{2+}_{aq} + HS^- \quad (10)$$

This mechanism is suitable for the explanation of the worsening of pitting corrosion in the presence of sulphide ions.

# 5. CONCLUSIONS

In the presented work, results from electrochemical measurements for AISI 304L and AISI 316L stainless steel in seawater at different temperatures (15, 25 and 35°C) and polluted with the sulphide ions in concentration of 10 and 40 ppm are reported.

- ✓ Increase in temperature of the seawater leads to the increase in corrosion attack of the investigated steels, which is manifested by the increase in corrosion current density and decrease in polarization resistance. The higher corrosion resistance was observed in AISI 316L stainless steel.
- ✓ Addition of sulphide ions to seawater leads to the worsening of the corrosion resistance of both steel materials. Once again, AISI 316L showed better results compared to the AISI 304L steel. The unfavorable effect of sulfide ions is explained by the adsorption of the $S^{2-}$ ions on the surface, which disturbs the growth of the oxide layer and decreases its effectiveness.
- ✓ Pitting corrosion is the dominant form of corrosion for AISI 304L and AISI 316L in clean and polluted seawater.
- ✓ The results of the optical profilometer measurements have shown that the diameter and pit depth strongly depend on the temperature and concentration of $S^{2-}$ ions in the solution.

# REFERENCES


1. *J. T. Black, R. A. Kohser*, DeGarmo's Materials and processes in manufacturing, John Wiley & Sons, Inc., New York, 2012.
2. *C.P. Dillon*, Corrosion resistance of stainless steels, Marcel Dekker, Inc., New York, 1995.
3. URL: https://www.unifiedalloys.com/blog/stainless-grades-families (5.8.2022.)
4. *Outokumpu*, Handbook of Stainless Steel, Outokumpu Oyj, Finland, 2013.
5. *I. Filipović, S. Lipanović*, General and inorganic chemistry, 2nd part, Školska knjiga, Zagreb, 1995.
6. URL:https://www.thetimes.co.uk/article/ancient-iron-beads-came-from-space-scientists-say-6lvt0kmf5lk (5.8.2022.)
7. *T. Rehren, T. Belgya, A. Jambon, G. Káli, Z. Kasztovszky, Z. Kis, I. Kovács, B. Maróti, M. Martinón-Torres, G. Miniaci, V. C. Pigott, M. Radivojević, L. Rosta, L. Szentmiklósi, Z. Szőkefalvi-Nagy*, 5000 years old Egyptian iron beads made from hammered meteoritic iron, Journal of Archaeological Science **40** (2013) 4785-4792. DOI: https://doi.org/10.1016/j.jas.2013.06.002
8. *W. Craig, A. Leonard*, Manufacturing Engineering, ED-Tech Press, 2021.
9. URL: https://www.steel.org/sustainability/ (5.8.2022.)
10. *W. Callister*, Fundamentals of Materials Science and Engineering, John Wiley & Sons, Inc., New York, 2001.
11. *J.R. Davis*, Alloying: Understanding the Basics, ASM International, Ohio, 2001
12. *I. Bačić*, Enhancement of corrosion protection of stainless steel by nanostructured sol-gel $ZrO_2$ films, Doctoral Thesis, University of Zagreb, Faculty of Science, 2016.
13. *D. Kvrgić*, Comparison of the corrosion behaviour of AISI 304, AISI 316L and duplex steel in chloride solution, Bachelor Thesis, University of Split, Faculty of Chemistry and Technology, 2018.
14. *M. Boniardi, A. Casaroli*, Stainless steels, Gruppo Lucefin, Esine, 2014
15. *K.H. Lo, C.H. Shek, J.K.L. Lai*, Recent developments in stainless steels, Materials Science and Engineering **65** (2009) 39-104. DOI: 10.1016/j.mser.2009.03.001
16. URL: https://patents.google.com/patent/US7905967B2/en (7.8.2022.)
17. *E. Carregueiro, T. Cremailh, K. Hasenclever, C. Herrera, B. Heritier, S. Jones, L. Peiro*, Martensitic Stainless Steels, International Stainless Steel Forum, 2021.

18. *R. N. Gunn*, Duplex Stainless Steels, Abington Publishing, Cambridge 1997.
19. URL: https://masteel.co.uk/news/what-is-duplex-and-super-duplex-stainless-steel/ (7.8.2022.)
20. *J.R. Davis*, Corrosion: Understanding the basics, ASM International, Ohio, 2000.
21. *A. Hrepić*, Corrosion inhibition of some metals by Padina pavonica (Linnaeus) Thivy extract, Bachelor Thesis, University of Split, Faculty of Chemistry and Technology, 2019.
22. *L. L. Shreir, R.A. Jarman, G.T. Burstein*, Corrosion Volume 1, Metal/Environment reactions, Butterworth Heinemann, Oxford, 1993.
23. *M. Metikoš-Huković, Elektrokemija*, University of Zagreb, Faculty of chemical engineering and technology, Zagreb, 2000.
24. *P.R. Roberge*, Corrosion Engineering: Principles and Practice, Mc Graw Hill, New York, 2008.
25. *E.E. Stansbury, R.A. Buchanan*, Fundamentals of Electrochemical Corrosion, ASM International, Ohio, 2000.
26. URL:https://www.degruyter.com/document/doi/10.1515/psr-2015-0006/html?lang=de (10.8.2022.)
27. *R. W. Revie*, Uhlig's Corrosion Handbook 3rd edition, John Wiley and Sons, USA, 2011.
28. URL:https://www.spec-net.com.au/press/1014/gaa_081014/Corrosivity-Zones-for-Steel-Construction-Galvanizers-Association (10.8.2022.)
29. *V. Martinac*, Mineral Raw Materials from Seawater, Internal script, University of Split, Faculty of Chemistry and Technology, 2019.
30. *H. A. Videla*, Biofilms and corrosion interactions on stainless steel in seawater, International Biodeterioration & Biodegradation **34** (1994) 245-257. DOI: https://doi.org/10.1016/0964-8305(94)90086-8
31. *J.R. Davis*, ASM Specialty Handbook: Stainless Steels, ASM International, Ohio, 1994.
32. URL:https://www.thefabricator.com/thefabricator/article/testingmeasuring/passivation-basics-will-this-stainless-steel-rust- (10.8.2022.)
33. *T. Brajković, I. Juraga, V. Šimunović*, Influence of surface treatment on corrosion resistance of Cr-Ni steel, Engineering Review **33** (2013) 129 – 134.

34. *J.W. Schultze, M.M. Lohrengel*, Stability, reactivity and breakdown of passive films. Problems of recent and future research, Electrochimica Acta **45** (2000) 2499-2513. DOI: https://doi.org/10.1016/S0013-4686(00)00347-9
35. *M. Zrinušić*, Influence of Chemical Surface Treatment of Stainless steels on Metal Ion Release, Master's thesis, University of Zagreb, Faculty of Mechanical Engineering and Naval Architecture, 2017.
36. *R. Baboian*, Corrosion Tests and Standards: Application and Interpretation, Second Edition, ASTM International, Baltimore, 2005.
37. URL: https://www.thoughtco.com/types-of-corrosion-2340005 (15.8.2022.)
38. *P.R. Roberge*, Corrosion Engineering: Principles and Practice, Mc Graw Hill, New York, 2008.
39. *H. Böhni*, Breakdown of passivity and localized corrosion processes, Langmuir **3** (1987) 924–930. DOI: https://doi.org/10.1021/la00078a010
40. *A. J. Sedriks*, Role of sulphide inclusions in pitting and crevice corrosion of stainless steels, International Metals Reviews **28** (1983) 295-307. DOI: https://doi.org/10.1179/imtr.1983.28.1.295
41. *M. S. Wiener, B. V. Salas, M. Quintero-Núñez & R. Zlatev* (2006) Effect of $H_2S$ on corrosion in polluted waters: a review, Corrosion Engineering, Science and Technology **41** (2006) 221-227. DOI:10.1179/174327806X132204
42. URL: https://www.ddcoatings.co.uk/2276/what-is-pitting-corrosion (20.8.2022.)
43. URL:https://www.materialsperformance.com/articles/corrosion-basics/2008/february/forms-of-corrosion (20.8.2022.)
44. URL:https://en.wikipedia.org/wiki/Intergranular_corrosion#/media/File:Intergranular_corrosion.JPG (20.8.2022.)
45. *M.F. McGuire*, Stainless Steels for Design Engineers, Austenitic Stainless Steel, ASM International, Ohio, 2008.
46. URL:https://mpelimited.co.uk/stainless-steel-advice-information/electropolishing-reduce-stress-corrosion-cracking (20.8.2022.)
47. *M. Horvat, I. Samardžić, V. Kondić,* Stress Corrosion, University of Varaždin, Mechanical Engineering Faculty Slavonski Brod, 2011.
48. URL: https://www.sunnyoptical.com/en/009006001/p400.html (20.8.2022.)

49. *M. S. Wiener, B. V. Salas, M. Quintero-Nunez and R. Zlatarev*, Effect of $H_2S$ on corrosion in polluted waters: a review, Corrosion Engineering, Science and Technology **41** (2006) 221-227. DOI: 10.1179/174327806X132204
50. *S. Yuan, B. Liang, S. O. Pehkonen*, Surface chemistry and corrosion behaviour of 304 stainless steel in simulated seawater containing inorganic sulphide and sulphate reducing bacteria, Corrosion Science **74** (2013) 353-366. DOI: 10.1016/j.corsci.2013.04.058
51. *P. Traverso, A.M. Beccaria, G. Poggi*, Effect of sulphides on corrosion of Cu-Ni-Fe-Mn alloy in seawater, British Corrosion Journal **29** (1994) 110-114. DOI: 10.1179/000705994798267881
52. *V. A. R. Boyapati, C. K. Kanukula*, Corrosion inhibition of Cu-Ni (90/10) alloy in seawater and sulphide polluted seawater environments by 1,2,3-benzotriazole, International Scholarly Research Notices **2013** (2013) 1-22. DOI: https://doi.org/10.1155/2013/703929
53. *H. Ma, X. Cheng, G. Li, S. Chem, Z. Quan, S. Zhao, L. Niu*, The influence of hydrogen sulphide on corrosion of iron under different conditions, Corrosion Science **42** (2000) 1669-1683. DOI: https://doi.org/10.1016/S0010-938X(00)00003-2
54. *F. Andreatta*, Local electrochemical behaviour of 7xxx aluminium alloys, PhD Thesis, University of Delft, Netherlands, 2004.
55. *W. S. Tait*, An introduction to electrochemical corrosion testing for practicing engineers and scientists, Pair O Docs Publications, Wisconsin, 1994.
56. *E. Stupnišek-Lisac*, Corrosion and construction material protection, University of Zagreb, Faculty of Chemical Engineering and Technology, 2007.
57. *E. B. Hansson, M. S. Odziemkowski, R. W. Gillham*, Formation of poorly crystalline iron monosulfides: surface redox reactions on high purity iron, spectroelectrochemical studies, Corrosion Science **48** (2006) 3767-3783. DOI: 10.1016/j.corsci.2006.03.010
58. *C. Leising*, Pitting corrosion measurement using 3D profilometry, Technical Report, 2014. DOI: 10.13140/RG.2.1.5098.3840
59. *I. Betova, M. Bojinov, O Hyokyvirta, T Saario*, Effect of sulphide on the corrosion behaviour of AISI 316L stainless steel and its constituent elements in simulated Kraft digester conditions, Corrosion Science **52** (2010) 1499-1507. DOI: 10.1016/j.corsci.2009.12.034